

FREQUENCY DOMAIN BLIND EQUALIZATION FOR
UPLINK SC-FDMA

BY

KABIRU OLUWASEUN AKANDE

A Thesis Presented to the
DEANSHIP OF GRADUATE STUDIES

KING FAHD UNIVERSITY OF PETROLEUM & MINERALS

DHAHRAN, SAUDI ARABIA

In Partial Fulfillment of the
Requirements for the Degree of

MASTER OF SCIENCE

In

ELECTRICAL ENGINEERING

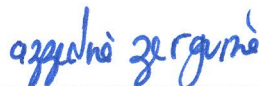
DECEMBER, 2014.

KING FAHD UNIVERSITY OF PETROLEUM & MINERALS
DHAHRAN 31261, SAUDI ARABIA

DEANSHIP OF GRADUATE STUDIES

This thesis, written by **KABIRU OLUWASEUN AKANDE** under the direction of his thesis adviser and approved by his thesis committee, has been presented to and accepted by the Dean of Graduate Studies, in partial fulfillment of the requirements for the degree of **MASTER OF SCIENCE IN ELECTRICAL ENGINEERING**.

Thesis Committee



Professor Azzedine Zerguine (Adviser)

(Co-adviser)



Dr. Wajih Abu-Al-Saud (Member)

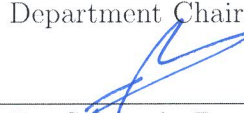


Dr. Samir Al-Ghadhban (Member)

(Member)



Dr. Ali Ahmad Al-Shaikhi
Department Chairman


Dr. Salam A. Zummo
Dean of Graduate Studies

Date

5/1/15



©Kabiru Oluwaseun Akande
2014

To my brother, Fakolujo Kehinde and his wife, Fakolujo Funmilayo.

ACKNOWLEDGMENTS

"...And if you were to count Allah's favors, you would not be able to...". I thank Almighty Allah for His everlasting blessings and favours on me for verily I least deserve them all.

Real gratitude goes to my parents and all the members of my family especially my brother and his wife for their support during a particularly challenging period of my life.

I deeply acknowledge the immeasurable contribution and generosity of my thesis adviser, Professor Azzedine Zerguine. I am grateful to my thesis committee members, Dr. Wajih Abu-Al-Saud and Dr. Samir Al-Ghadhban, for their constructive suggestions. I owe many thanks to Dr Naveed Iqbal for his numerous technical contributions and for having a good sense of humor.

Special thanks goes to KFUPM and DGS for the prestigious scholarship offered to me for this MS program.

Finally, I appreciate the ever presence of the KFUPM Nigerian community, they made my experience in KFUPM home away from home. To all the faceless contributors, I can not thank you enough.

TABLE OF CONTENTS

LIST OF TABLES	viii
LIST OF FIGURES	ix
LIST OF ABBREVIATIONS	xi
ABSTRACT (ENGLISH)	xv
ABSTRACT (ARABIC)	xvii
CHAPTER 1 INTRODUCTION	1
1.1 Motivation	1
1.2 The need for Equalization	4
1.3 Adaptive Equalization	4
1.4 Non-Blind (Trained) Equalization	6
1.5 Blind Equalization	7
1.6 Outline and Contribution	9
CHAPTER 2 BACKGROUND INFORMATION	10
2.1 Introduction to SC-FDMA	10
2.2 Mathematical Description of SC-FDMA	13
2.3 Single Carrier-Frequency Domain Equalization	18
2.4 Summary	20
CHAPTER 3 BLIND ALGORITHMS	21

3.1	Introduction to Blind Algorithms	21
3.2	Constant Modulus Algorithm (CMA)	23
3.2.1	Godard dispersion constant	26
3.3	MultiModulus Algorithm (MMA)	26
3.4	Soft Constraint Satisfaction Multimodulus Algorithm (SCS-MMA)	28
3.5	Summary	30
CHAPTER 4 FREQUENCY DOMAIN BLIND ALGORITHMS		31
4.1	Introduction to FD Implementation	31
4.2	Overlap-Save Convolution Method	34
4.3	Computational Complexity	40
4.4	Performance Measures	42
4.4.1	Mean Square Error (MSE)	43
4.4.2	Inter-symbol Interference (ISI)	44
4.4.3	Symbol Constellation	45
4.4.4	Bit Error Rate	45
4.5	Simulation Results	46
4.6	Summary	50
CHAPTER 5 FDSCS-MMA FOR SCFDMA		53
5.1	Introductiocomn to FDBE-SC-FDMA	53
5.2	NFDSCS-MMA without Overlap-Save Technique	54
5.3	Simulation results	57
5.3.1	Experiment 1	57
5.3.2	Experiment 2	65
5.4	Summary	72
CHAPTER 6 CONCLUSION AND FUTURE WORK		76
6.1	Conclusion	76
6.2	Future work	77
REFERENCES		78

LIST OF TABLES

3.1	Blind Algorithms Cost Functions	30
3.2	Blind Algorithms Estimation Errors	30
4.1	Number of Real Multiplications for Varying Equalizer Length . .	41

LIST OF FIGURES

1.1	Constellation plots showing equalization effect	5
1.2	A typical baseband communication system for blind equalization .	8
2.1	Block diagram of SC-FDMA system.	14
3.1	CMA cost function surface [30]	25
4.1	Normalized NFDSCS-MMA equalizer with overlap-save method. .	39
4.2	Comparison of computational complexity for varying length of equalizer.	42
4.3	MSE convergence comparison for equalizer length $N = 64$, SNR=10dB.	43
4.4	MSE convergence comparison for equalizer length $N = 64$, SNR=20dB.	44
4.5	MSE convergence comparison for equalizer length $N = 64$, SNR=30dB.	45
4.6	Residual ISI convergence curves for equalizer length $N = 64$, SNR=10dB.	46
4.7	Residual ISI convergence curves for equalizer length $N = 64$, SNR=20dB.	47
4.8	Residual ISI convergence curves for equalizer length $N = 64$, SNR=30dB.	48
4.9	MSE convergence comparison for equalizer length $N = 128$	49
4.10	MSE convergence comparison for equalizer length $N = 256$	50

4.11	Residual ISI convergence curves for equalizer length $N = 128$. . .	51
4.12	Residual ISI convergence curves for equalizer length $N = 256$. . .	52
5.1	Block diagram of FD equalizer.	56
5.2	Normalized FDSCS-MMA algorithm.	58
5.3	MSE curves for unnormalized FD blind algorithms.	59
5.4	MSE curves for normalized FD blind algorithms.	60
5.5	MSE comparison curves for FD blind algorithms.	61
5.6	MSE comparison curves for FD blind algorithms, SNR=10dB. . .	62
5.7	MSE comparison curves for FD blind algorithms, SNR=30dB. . .	63
5.8	MSE comparison curves for mapping scheme.	64
5.9	MSE comparison curves for normalized FD blind algorithms. . . .	65
5.10	Constellation without a carrier offset.	66
5.11	MSE comparison curves for blind algorithms, SNR=10dB.	67
5.12	MSE curves comparison between NFDSCS-MMA and FDSCS-MMA, SNR=20dB.	68
5.13	MSE comparison curves for blind algorithms, SNR=20dB.	69
5.14	Residual ISI convergence curves for 4-QAM for blind algorithms, SNR=10dB.	70
5.15	Residual ISI convergence curves for 4-QAM for blind algorithms, SNR=20dB.	71
5.16	Residual ISI convergence curves for 4-QAM for blind algorithms, SNR=30dB.	72
5.17	Residual ISI convergence curves for 64-QAM for blind algorithms, SNR=20dB.	73
5.18	Constellation without a carrier offset, SNR=20dB.	74
5.19	Constellation without a carrier offset, SNR=30dB.	74
5.20	BER comparison of NFDSCS-MMA and Linear MMSE.	75

LIST OF ABBREVIATIONS

3GPP	3rd Generation Partnership Project
ATM	Asynchronous Transfer Mode
BER	Bit Error Rate
BPSK	Binary Phase Shift Keying
CMA	Constant Modulus Algorithm
CP	Cyclic Prefix
CPSCS	Cyclic-Prefixed Single Carrier System
DFDMA	Distributed Frequency Domain Multiple Access
DFE	Decision Feedback Equalizer
DFT	Discrete Fourier Transform
FB	Feedback Filter
FD	Frequency Domain
FD-SCA	Frequency Domain Square Contour Algorithm

FDDE-SC-FDMA	Frequency Domain Blind Equalization of SC-FDMA
FDSCS-MMA	Frequency Domain Soft Constraint Satisfaction Multimodulus Blind Algorithm
FF	Feedforward Filter
FFT	Fast Fourier Transform
FTTC	Fiber-To-The-Curb
IBI	Interblock Interference
IFDMA	Interleaved Frequency Domain Multiple Access
IFFT	Inverse Fast Fourier Transform
ISI	Inter-symbol Interference
LAN	Local Area Network
LE	Linear Equalizer
LFDMA	Localized Frequency Domain Multiple Access
LMS	Least Mean Square
LTE	Long-time Evolution
M-QAM	M- Quadrature Amplitude Modulation
MCMA	Modified Constant Modulus Algorithm

MIMO	Multiple-Input Multiple-Output
MLSE	Maximum-Likelihood Sequence Estimation
MMA	MultiModulus Algorithm
MMSE	Minimum Mean Square Error
MSE	Mean Square Error
NFDSCS-MMA	Normalized Frequency Domain Soft Constraint Satisfaction MultiModulus Blind Algorithm
OFDM	Orthogonal Frequency Multiple Access
OFDMA	Orthogonal Frequency Multiple Access Scheme
PAPR	Peak to Average Power Ratio
QAM	Quadrature Amplitude Modulation
QPSK	Quadrature Phase Shift Keying
RB	Resource Block
RCA	Reduced Constellation Algorithm
RLS	Recursive Least Square
SC-FDE	Single Carrier Frequency Domain
SC-FDMA	Single Carrier Frequency Division Multiple Access

TD	Time Domain
UMTS	Universal Mobile Telecommunications System
VDSL	Video Digital Subscriber Line
ZF	Zero-forcing

THESIS ABSTRACT

NAME: KABIRU OLUWASEUN AKANDE
TITLE OF STUDY: FREQUENCY DOMAIN BLIND EQUALIZATION FOR
UPLINK SC-FDMA
MAJOR FIELD: ELECTRICAL ENGINEERING
DATE OF DEGREE: DECEMBER, 2014

Single Carrier Frequency Division Multiple Access (SC-FDMA) has been adopted and employed as the standard in the 3rd Generation Partnership Project (3GPP) LTE (Long-term Evolution) uplink multiple access scheme. It offers comparable performance and complexity to Orthogonal Frequency Division Multiple Access Scheme (OFDMA) but has lower peak to average power ratio (PAPR), offering to mobile terminals power-efficient transmission and longer battery life. However, due to its single carrier nature, SC-FDMA performance degrades in channels with long impulse response and becomes prohibitive to equalize in time domain (TD). Furthermore, of the 7 SC-FDMA symbols in the LTE uplink slot, one full symbol (training symbol) is used for channel estimation leading to about 14% throughput degradation. In this work, a frequency domain soft constraint satisfaction

multimodulus blind algorithm (FDSCS-MMA) is developed and proposed for the equalization of SC-FDMA system. The frequency domain approach results in computational complexity reduction while blind implementation, which avoids the use of training symbols, ensured improved spectral efficiency and throughput. The algorithm convergence is further improved by normalizing each of the frequency bins in the weight update. Simulation results show superior performance of the developed algorithm over other blind algorithms in terms of faster convergence rate and lower residual mean square error (MSE). The proposed algorithm achieves a slightly lower bit error rate (BER) performance compared to zero-forcing (ZF) algorithm and minimum mean square error (MMSE). The results obtained suggest that SC-FDMA can be equalized in broadband wireless systems, characterized by a long channel impulse response, using the proposed algorithm with substantial throughput improvement.

الاسم: كابيرو أكاندي

عنوان الأطروحة: التنقية العمياء للموجات الصاعدة في المجال الترددي

التخصص: الهندسة الكهربائية

التاريخ: ديسمبر 2014

لقد اعتمدت تقنية التقسيم الترددي لحامل الإشارة المنفرد متعددة الوصول (SC-FDMA) و استخدمت من قبل الجيل الثالث من مشروع الشراكة (3GPP) كطريقة نموذجية لإرسال الإشارات الصاعدة. هذه التقنية توفر أداء مشابها لتقنية التقسيم الترددي للإشارات المتعددة الوصول (OFDMA) لكنها تتميز بنسبة أعلى طاقة لمعدل طاقة (PAPR) أقل، مما يوفر لأجهزة الاتصال المتنقل إريالا موفرا للطاقة و فترة حياة أطول للبطارية. لكن بسبب اعتمادها على حامل إشارة منفرد، فإن أداء هذه التقنية ينخفض في القنوات ذات الاستجابة النبضية الممتدة و يصبح من الصعب تنقيتها في المجال الزمني. بالإضافة إلى ذلك، فإن واحدا من كل سبعة إشارات مرسله في نطاق زمني واحد يتم استخدامها في استكشاف القناة، و هذه يؤدي إلى هبوط في سرعة الإرسال الفعلية بنسبة أربعة عشر بالمئة. في هذه الأطروحة، نقترح خوارزمية عمياء متعددة المعاملات بحد إرضاء مرن للتنقية في المجال الترددي تتطلب وقتا أقل للحصول على نتيجة مرضية بينما التنفيذ الأعمى، الذي يتفادى استعمال إشارات التمرين، يضمن تحسن السرعة الفعلية و فعالية استخدام الطيف الترددي. سرعة وصول الخوارزمية للنتيجة المطلوبة يتم تحسينها عن طريق تسوية كل الوحدات الترددية أثناء تحديث الوزن لكل وحدة. التجارب باستخدام الحاسوب تظهر أداء أقوى للخوارزمية المقترحة بالمقارنة مع الخوارزميات العمياء الأخرى من حيث سرعة الوصول للنتيجة المطلوبة و تقليل الخطأ. الخوارزمية المقترحة تحقق معدل خطأ (BER) أقل بقليل من تقنية فرض الصفر (Zero Forcing) و تقنية الحد الأدنى للخطأ التربيعي (MSE). النتائج المتوفرة تشير إلى أن الإشارات الصاعدة يمكن تنقيتها في أنظمة الاتصالات اللاسلكية عريضة الموجة باستخدام الخوارزمية المقترحة مع تحسن جوهري في سرعة نقل البيانات الفعلية

CHAPTER 1

INTRODUCTION

1.1 Motivation

The demand for high data transmission rates have been on the rise in recent years with organizations and individuals requiring ultra high-speed data transmission scheme. Broadband wireless transmission is employed in delivering this high speed data requirement to subscribers in a very hostile radio environment which offers multipath to transmitted signal. The multipath could be severe requiring sophisticated corrective measures at the receiver. The majority of todays commercially available digital cellular communication systems are covered in details by specified standards. However, one of the most critical parts, namely the data receiver, is specified in terms of performance only, thus leaving room for manufacturers and operators to implement individual solutions. This motivates the investigation of complexity and performance of various receiver structures. OFDMA is a popular technique which uses a low symbol rate modulation specially

designed to cope with severe channel conditions in multipath environment [1]. However, it has high peak to average power ratio (PAPR) which imposes high power penalty on mobile users [2].

Single carrier frequency domain multiple access scheme (SC-FDMA) is a variant of orthogonal frequency domain multiple access (OFDMA) with an additional discrete Fourier transform (DFT) processing block hence is referred to as DFT-coded OFDMA [3]. It has been adopted in Third Generation Partnership Project (3GPP) Long-Term Evolution (LTE) uplink scheme due to its lower PAPR while maintaining comparable performance and complexity to OFDMA [4, 5]. The lower PAPR feature makes it suitable for uplink communication benefiting mobile users in terms of low cost and improved power-efficient transmission [4]. SC-FDMA can be viewed as an OFDMA system preceeded by a DFT block but in contrast to OFDMA, it is a single carrier system as the name implies [6]. Maximum-Likelihood Sequence Estimation (MLSE) is known to be the optimum equalization algorithm for single carrier but its computational complexity grows exponentially in channels with long impulse response and large delay spread. This makes it computationally prohibitive to use in broadband wireless systems. Moreover, MLSE is implemented in time-domain and as such, it is unsuitable for SC-FDMA equalization [6]. This is due to the fact that SC-FDMA technique is set up in frequency domain and it is easier to implement its equalization in frequency domain as this avoids a lot of complications [7].

In the LTE uplink, one full training SC-FDMA symbol (preamble) is used

followed by 6 data symbols (with no training). The channel is estimated (e.g. using least squares) using this single training symbol. Currently, Zero-forcing (ZF) algorithm is used to equalize SC-FDMA in frequency domain with the aid of regular pilots insertion for channel estimation [7, 8]. The problem with this equalization approach is that it leads to throughput degradation of about 14% in each uplink slot since 1 out of 7 SC-FDMA symbols is used as training symbol. Therefore, this work presents a frequency domain implementation of soft-constraint satisfaction multimodulus blind algorithm (FDSCS-MMA) for equalization of SC-FDMA to reduce this degradation and substantially improve the spectral efficiency and throughput.

The proposed frequency domain implementation is based on the SCS-MMA [9] which was derived by applying the principle of soft-constraint satisfaction to relax the constraints in Lin's cost function [10]. This algorithm avoids the use of training symbols in order to improve the spectral efficiency and throughput. Also, the FD implementation greatly reduces the computational complexity associated with time domain implementation in channels with long impulse response. Furthermore, FDSCS-MMA convergence is greatly improved by normalizing each of the frequency bins in the weight update to realize normalized FDSCS-MMA (NFDSCS-MMA). Finally, NFDSCS-MMA achieves better performance than both the FD modified constant modulus algorithm (NFDMMMA) [12] and the popular constant modulus algorithm (CMA) in terms of faster convergence and lower residual MSE.

1.2 The need for Equalization

Broadband wireless transmission channel used in meeting high data transmission rates demand offers multipath to transmitted signal. Multipath is the phenomenon describing the arrival of transmitted symbols at the receiver from two or more paths and it causes interference and phase shifting in the resulting signal. An equalizer is the device used for implementing the correction required in the received symbols. It forms a significant part of modern digital communication system as signals are transmitted at higher signaling rates leading to increased distortion in the transmitted symbols. Therefore, an equalizer acts as a counter-measure to the effects of the channel and as a result, accurate decisions can be made by the receiver.

Figure 1.1 shows the effect of equalization. It recovers the transmitted symbols by opening the eye of the received constellation.

1.3 Adaptive Equalization

Equalizers are realized as digital filters for implementation purpose. The coefficients of the filter are referred to as the equalizer taps because the filter is realized as a tapped delay line. Tapped delay line stores delayed versions of the input signal which is multiplied by the taps of the filter. In this manner, optimum

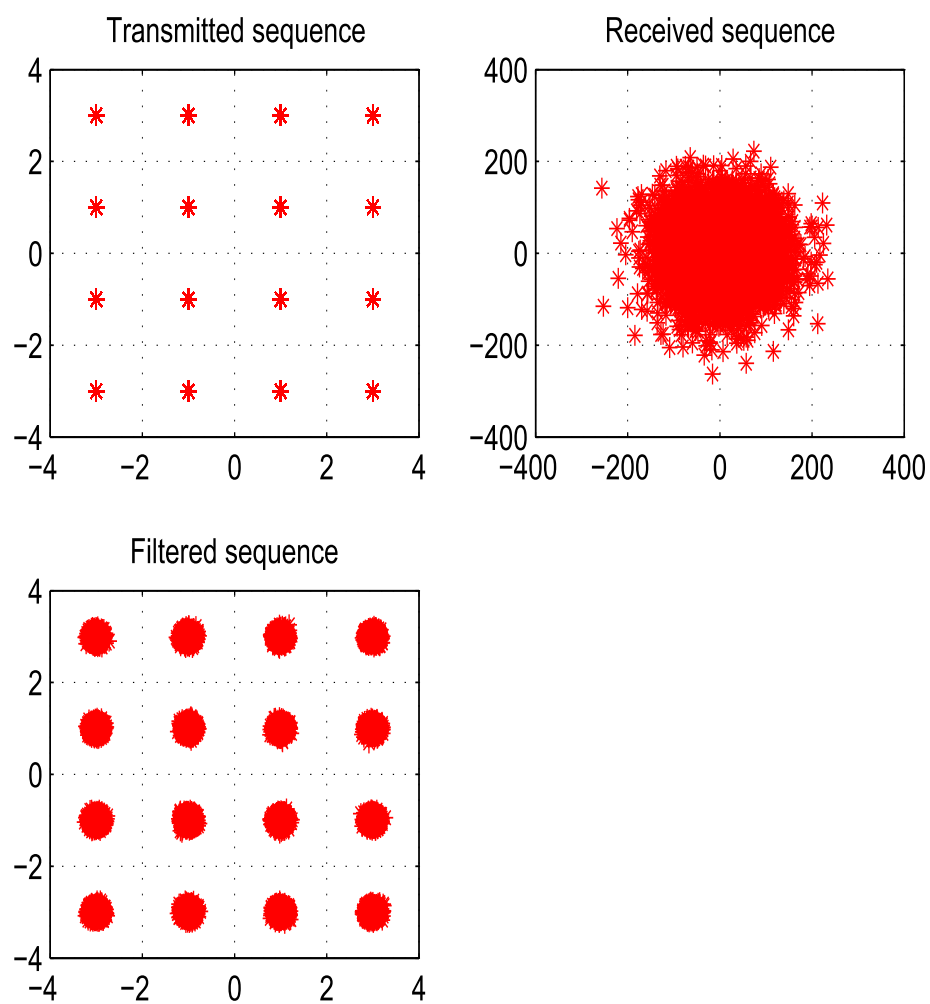


Figure 1.1: Constellation plots showing equalization effect

values of the filter taps can be arrived at after some computations. Due to the varying nature of the channel characteristics, the optimum settings of the filter coefficient at time t might not be optimum at time $(t + \delta)$. Hence, there is need to adaptively compute and adjust the optimum settings of the filter taps to suit each arriving signal. This is done using adaptive techniques which leads to the design of adaptive equalizers.

Adaptation leads to variation of the filter coefficients as time progresses and the adaptive equalizer adapts to the varying channel characteristics. The equalizer taps are usually initialized at some random value, zeros for non-blind filter and mostly, center-spike initialization is used for blind algorithms. The equalizer then makes changes to the initial tap values by updating itself with some measures of error derived from the cost function of the adapting algorithm. The error serves as an adjustment factor through which each tap is updated until the equalizer ideally converges. The ideal convergence is obtained when the convolution between the channel impulse response and that of the equalizer equals one. This is known as the steady state of the equalizer and any changes at this stage in the channel characteristics can be tracked by the equalizer and its taps adjusted accordingly.

1.4 Non-Blind (Trained) Equalization

Trained equalizers derive their error from the difference between the equalizer output and an ideal reference signal. The ideal reference signal is usually a copy of the transmitted symbol made available to the receiver during a training phase.

The majority of the equalizers employed in practice operate on this technique. The training sequence are transmitted intermittently to cater for time-varying characteristics of the channel, hence the bandwidth consumption increased in a highly dispersive channel as retransmission occurs more frequently. The most popular algorithm used for trained equalization is the Least Mean Square (LMS) algorithm which operates by comparing the output of the equalizer to a corresponding training sequence. The error generated from this comparison is then used by the equalizer taps to adaptively move towards the minimum point on the error surface and generally reduce the error.

The major drawback of this approach is the bandwidth consumption caused by transmission of training sequence and this leads to inefficient spectral usage. The inefficiency gets worse in highly time-varying channels where re-transmission of the training sequence becomes frequent.

1.5 Blind Equalization

Blind equalizers operate without the aid of an ideal reference hence they achieve equalization without using training sequence. Blind equalization is employed mostly in data communication for start-up to provide initial convergence for adaptive equalizer. It is also used in situations where sending training sequence might be impractical. An example of this in practice is the equalization adopted by digital television provider. They send out constant data streams to multitude of users who connect and disconnect at will. Frequent retransmission of training

sequence will severely deplete the available bandwidth for useful symbols so an alternative technique is required to achieve equalization without the use of training sequence. A typical baseband communication system for blind equalization is shown in Fig.1.2.

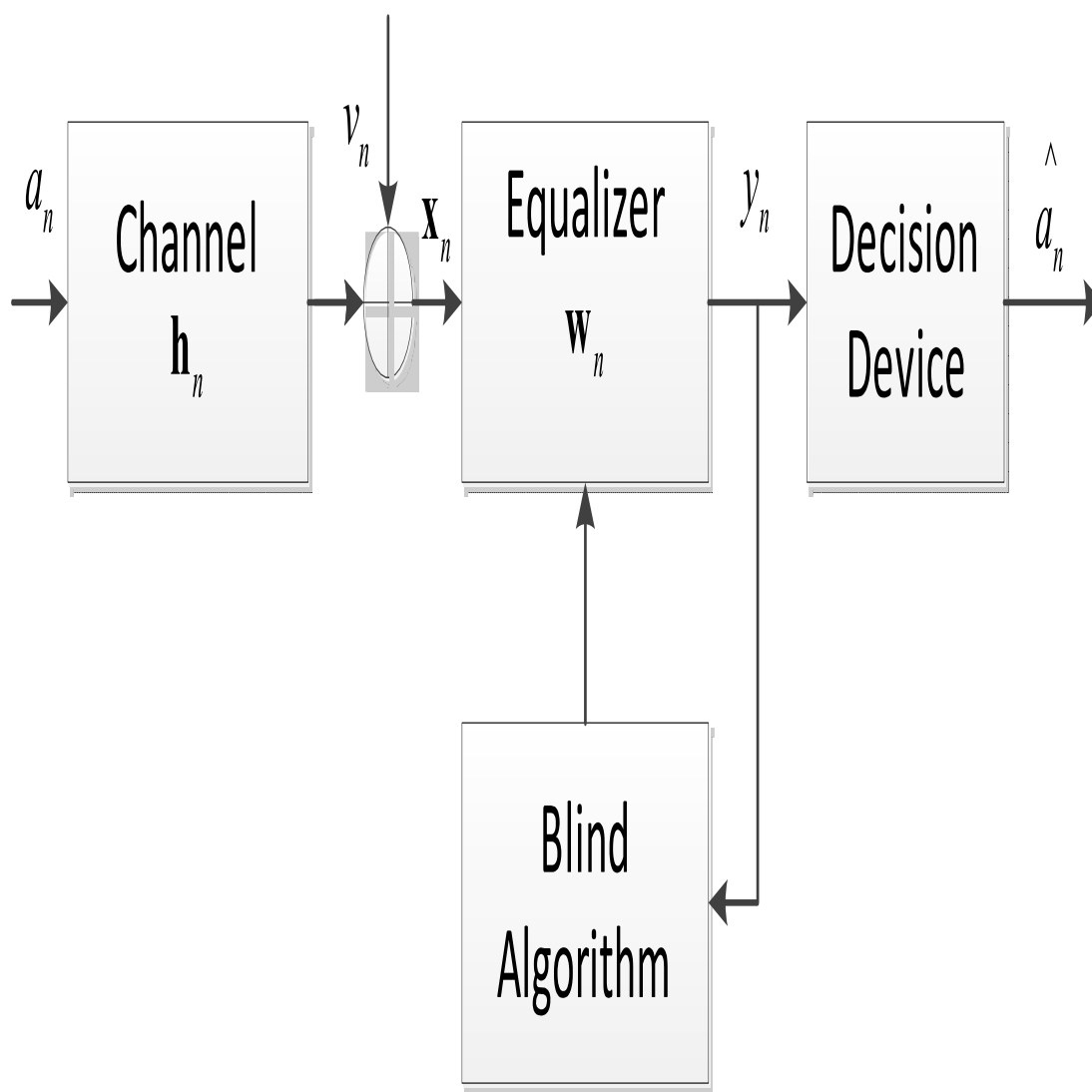


Figure 1.2: A typical baseband communication system for blind equalization

1.6 Outline and Contribution

The layout of the thesis is as follows: Chapter 2 gives the details of SC-FDMA modulation format, its mathematical structure and various equalization techniques already proposed for it. Chapter 3 discusses time-domain description of blind algorithms. Chapter 4 compares time-domain SCS-MMA with its frequency domain implementation in terms of computational complexity, mean square error (MSE), inter-symbol interference (ISI) and bit error rate (BER). Chapter 5 adapts the proposed algorithm to SC-FDMA equalization and its performance is compared to those of the other popular blind algorithms. Chapter 6 concludes the thesis and gives recommendations for further work.

CHAPTER 2

BACKGROUND

INFORMATION

2.1 Introduction to SC-FDMA

3GPP set up a program in late 2004 to keep universal Mobile Telecommunications System(UMTS) at the forefront of mobile wireless for future generation of mobile communications. The key objectives of the project were improvement of throughput, spectrum efficiency, latency, complexity, channel bandwidth and implementation cost. 3GPP resulted in a completely new air interface, based essentially on orthogonal frequency division multiplexing (OFDM), at the conclusion of the program [3].

OFDM is the underlining modulation technology for LTE systems. Advancements in digital signal processing made the adoption of OFDM possible as the initial reluctance was processing power stemming from the Fast Fourier Transform

(FFT) operations involved in OFDM generation.

OFDM offers resistance to the distortion caused by multipath delay spread (fading) in the radio channel. Multipath causes inter-symbol interference (ISI) in the received signal if adequate measures are not taken to address its effects. The insertion of cyclic prefix or guard period between transmitted OFDM symbols, the length of which should be equal to the multipath components of the channel for its effectiveness, helps in avoiding ISI in multipath environment. OFDM easily adapt to frequency and phase distortions in the received signal by embedding in its symbols, pilots of predetermined amplitude and phase.

The advantages of OFDM include transmitting low-rate symbols with ability to withstand multipath effects and an inherent frequency domain processing which simplifies correction of received signal errors. However, OFDM is susceptible to two major disadvantages. First is the fact that as its subcarriers increase, they add up to sinc-like waves with significantly high PAPR. The high PAPR causes spectral regrowth in the adjacent channels and is very costly to design an amplifier able to deal efficiently with it. The second significant issue with OFDM is loss of orthogonality resulting from tight spacing of subcarriers. The problems resulting from loss of orthogonality include spread of energy over subsequent subcarriers, phase-noise-induced ISI and boomerang effect of Doppler shift. The disadvantages of OFDM led to a proposal of a new modulation scheme referred to as single carrier frequency division multiple access (SC-FDMA) [8].

SC-FDMA combines both the advantages of OFDM and that of single carrier.

It has the low PAPR of single-carrier systems and the multipath resistance of OFDM. Basically, the real LTE signal is made up of a resource block (RB) containing 12 adjacent subcarriers ($15kHz$ each) lasting for about $0.5\mu s$ and containing seven SC-FDMA symbols. The basic difference between OFDMA (multiple access version of OFDM) and SC-FDMA scheme is that OFDMA transmit N symbols in parallel, one symbol per subcarrier while SC-FDMA does it in series with each symbol spread out over the assigned subcarriers. The low PAPR of SC-FDMA is due to the extra FFT/IFFT processing inserted into its block. OFDMA typically modulates each subcarrier with a unique data symbol resulting in a one-to-one mapping between subcarrier and data symbol. Then an inverse FFT is performed to realize time-domain signals. These are then summed to get the final transmitted time-domain waveform. However, the sum of time-domain signals approaches Gaussian noise statistics with increasing number of subcarriers due to the random nature of modulating data. Hence, PAPR of OFDMA increases with increasing number of subcarriers.

This is not the case in SC-FDMA because a basic difference is that rather than modulate the subcarrier in SC-FDMA directly with modulating symbols, it is the DFT of the modulating symbols that is used. This ensures that each subcarrier carries a little of the frequency domain representation of each of the modulating symbols, rather than the symbols themselves, which is where the single carrier in SC-FDMA originates. Hence, the peak to average ratio (PAR) of SC-FDMA remains as that of the original data symbols. The constant nature of the subcarriers

over an SC-FDMA period enables SC-FDMA to maintain its protection against multipath interference. Therefore, SC-FDMA has all the benefits of OFDMA, including the multipath protection, without high PAPR issue. Hence, it is identified as a better option for LTE uplink especially considering power constraint of mobile terminals.

2.2 Mathematical Description of SC-FDMA

SC-FDMA is a multi-access single carrier modulation technique with a frequency domain equalization at the receiver and allows parallel transmission of multiple user data. It is a variant of OFDMA with an additional DFT and IDFT processing block at the transmitter and receiver respectively. What follows in this section is a detailed treatment of this well-known scheme. As stated in [6], it is advantageous to set up our system in terms of matrices as this simplifies implementation, provides a clear understanding of the system and eases many performance analyses. Hence, our system is set up in this manner with the block diagram shown in Fig. 2.1. In order to form an SC-FDMA block, sequence of data bits $\{a_n\}$ are first modulated into symbols using any of the modulation methods (BPSK, QPSK or M-QAM). For q^{th} user, where Q represents the total number of users in the system, data block \mathbf{x} consisting of N symbols, is generated from the resulting modulation scheme as

$$\mathbf{x} = [x_0, x_1, \dots, x_{N-1}]^T \quad (2.1)$$

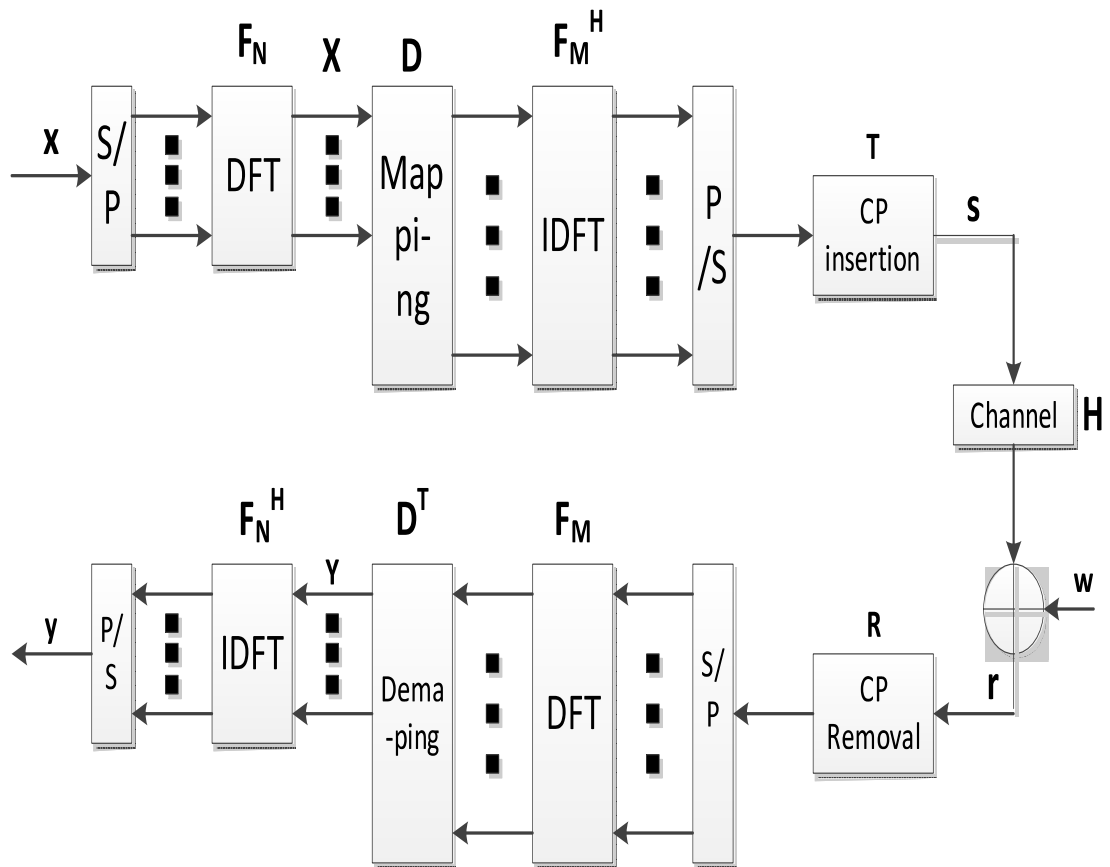


Figure 2.1: Block diagram of SC-FDMA system.

where $[\cdot]^T$ denotes transpose operation.

The N -point discrete Fourier transform (DFT) of \mathbf{x} is taken as

$$\mathbf{X} = \mathbf{F}_N \mathbf{x} \quad (2.2)$$

to yield frequency coefficients which are then assigned orthogonal subcarriers for transmission over the channel. From the DFT operation, \mathbf{X} represent DFT outputs for q^{th} user given as

$$\mathbf{X} = [X_0, X_1, \dots, X_{N-1}]^T \quad (2.3)$$

while \mathbf{F}_N is an $N \times N$ DFT matrix defined as

$$(\mathbf{F}_N)_{j,k} = \left(\frac{1}{\sqrt{N}} e^{-i \frac{2\pi}{N} jk} \right), j, k = 0, \dots, N-1 \quad (2.4)$$

The $\frac{1}{\sqrt{N}}$ is a normalization factor to ensure the same signal output power. There are two ways of assigning subcarriers in SC-FDMA. When adjacent subcarriers are allocated to DFT outputs from the same user such that the user data are confined to only a fraction of the available bandwidth, this is referred to as localized SC-FDMA (LFDMA) but when DFT outputs are spread over the entire bandwidth with zero amplitude allocated to unused subcarriers, it is referred to as distributed SC-FDMA (DFDMA). A special case of DFDMA is interleaved SC-FDMA (IFDMA) where the occupied subcarriers are equally spaced. The al-

location schemes can be implemented using a resource allocation matrix \mathbf{D} given in [6]. After allocating the subcarriers, M-point ($M > N$) inverse DFT (IDFT) is taken to convert the signal to time domain. The resulting signal is given as

$$\mathbf{S} = \mathbf{F}_M^H \mathbf{X} \quad (2.5)$$

where \mathbf{S} is the k^{th} SC-FDMA symbol consisting of all the users' signal

$$\mathbf{S} = [S_0, S_1, \dots, S_{M-1}]^T \quad (2.6)$$

while \mathbf{F}_M^H is an $M \times M$ IDFT matrix and \mathbf{H} is an Hermitian operator. The total number of users in the SC-FDMA system equals bandwidth expansion factor $Q = M/N$ and M is the total number of subcarriers. In order to complete an SC-FDMA block, the time domain signal is converted from parallel to serial arrangement and is cyclically extended by addition of cyclic prefix. A cyclic prefix (CP), which is typically removed at the receiving section before any major processing, is obtained by prefixing a symbol with its tail end to achieve mainly two purposes. If the CP length is the same or longer than the length of multipath channel delay spread, it helps prevent interblock interference (IBI) and also enable convolution between the channel impulse response and transmitted signal to be modeled as circular as opposed to linear convolution. This makes frequency domain equalization easy at the receiver. It is this second purpose we have taken advantage of in adapting the FD blind algorithms to equalizing SC-FDMA symbols. The

transmitted SC-FDMA block is

$$\mathbf{S} = [S_{M-P}, \dots, S_{M-2}, S_{M-1}, S_0, S_1, \dots, S_{M-1}]^T \quad (2.7)$$

where P is the length of the prepended CP. In matrix format, both the transmitted and received signal can be respectively written as

$$\mathbf{S} = \mathbf{T}\mathbf{F}_M^H\mathbf{D}\mathbf{F}_N\mathbf{x} \quad (2.8)$$

and

$$\mathbf{Y} = \mathbf{H}\mathbf{S} + \mathbf{V} \quad (2.9)$$

We define \mathbf{T} and \mathbf{R} which are used in adding and removing CP, respectively, as

$$\mathbf{T} \triangleq \begin{bmatrix} \mathbf{I}_{P \times M} \\ \mathbf{I}_M \end{bmatrix}, \mathbf{R} \triangleq \begin{bmatrix} \mathbf{O}_{M \times P} & \mathbf{I}_M \end{bmatrix} \quad (2.10)$$

In (2.10), $\mathbf{I}_{P \times M}$ is a matrix used in copying the last P row of \mathbf{I}_M , $\mathbf{O}_{M \times P}$ is an $M \times P$ zero matrix and \mathbf{I}_M is an $M \times M$ identity matrix. \mathbf{H} is $(P+M) \times (P+M)$ channel matrix and \mathbf{V} is $(P+M) \times 1$ noise vector. The received signal undergo the reverse of what it has undergone during the transmitting phase as shown in Fig. 2.1, hence the input to the equalizer is

$$\mathbf{Y}' = \mathbf{H}'\mathbf{x} + \mathbf{V}' \quad (2.11)$$

where \mathbf{H}' is an $N \times N$ diagonal matrix containing the channel frequency response for the q^{th} user and \mathbf{V}' is the effective $1 \times N$ noise vector. They are given as

$$\mathbf{H}' = \mathbf{F}_N^H \mathbf{D}^T \mathbf{F}_M (\mathbf{R} \mathbf{H} \mathbf{T}) \mathbf{F}_M^H \mathbf{D} \mathbf{F}_N \quad (2.12)$$

and

$$\mathbf{V}' = \mathbf{F}_N^H \mathbf{D}^T \mathbf{F}_M \mathbf{R} \mathbf{V} \quad (2.13)$$

This result from the fact that addition and removal of CP turns channel matrix into a circulant matrix and the resulting circulant matrix is diagonalized by DFT processing [13].

2.3 Single Carrier-Frequency Domain Equalization

The majority of the work that has been done on SC-FDMA equalization has been confined to consideration of non-adaptive non-linear equalizers. Both [14] and [15] proposed a decision feedback equalizer (DFE) structure for single carrier frequency domain equalization (SC-FDE-DFE). The feedforward filter (FF) was implemented in frequency domain while the feedback filter (FB) was in time domain. The same technique was extended by [16] to FDE multiple-input multiple-output (FDE-MIMO) systems. Iterative block DFE was introduced by [17] in which decisions are iterated over before being fed back into the

equalizer. The iterative procedure ensures that more reliable decisions are used as feedback and this improve the efficiency of the feedback filter.

SC-FDE was extended to SC-FDMA by [6] with the same structure of frequency domain forward filter and time-domain feedback filter. SC-FDE-DFE was proposed for multi-user SC-FDMA by [18] where complexity was reduced by avoiding matrix inversion. Blind time domain linear equalizer (TD-LE) structure was proposed in [7] and [19] to reduce degradation of throughput. Zero-forcing technique was combined with MMSE criterion to achieve an equalization without the need for channel estimation. While this solved the spectral efficiency and throughput problem, the time domain implementation is not suitable for channels with long impulse response and large delay spread as the complexity will be very high. The author further proposed an adaptive FD-DFE for SC-FDMA in [20] using least mean square algorithm. The use of encoder and decoder together with the DFE implementation still result in high complexity. Adaptive FD-DFE was proposed by [21] using recursive least square (RLS) for the equalizer adaptation. Both FF and FB are adapted in frequency domain and this greatly reduce complexity though it is still DFE implementation with use of training symbols.

A critical survey of the literature as reviewed above shows a trend in the work done on SC-FDMA equalization. A pervasive and recurrent theme in the equalizer design approach is the use of DFE. The equalizers consist of non-adaptive FD-DFE which is an extension form SC-FDE-DFE, non-adaptive blind TD-LE and adaptive non-blind FD-DFE. There has been no investigation of frequency

domain adaptive blind linear equalization for SC-FDMA hence, this work is focused on this area.

The advantages are reduced complexity offered by linear frequency domain implementation together with improved throughput and spectral efficiency resulting from blind equalization. The throughput gain from implementing this algorithm for SC-FDMA amounts to about 14% increase.

2.4 Summary

In this chapter, SC-FDMA fundamentals have been discussed including its advantages over OFDMA. The mathematical structure of SC-FDMA was presented along with the various equalizers proposed for it in the literature.

A gap was identified in the form of throughput degradation and will be addressed in the remaining chapters of this work.

CHAPTER 3

BLIND ALGORITHMS

3.1 Introduction to Blind Algorithms

Blind algorithms are very different from their non-blind counterparts and their formulation is fundamentally different. In non-blind algorithms, the cost function is formulated as a minimization of the error between the output of the equalizer and an ideal reference signal (if this is available) or the slicer's output. A slicer is a decision device which takes output of the equalizer as an input then maps it onto a nearest point on the source signal constellation space. An example of non-blind algorithm is the popular least mean square (LMS) algorithm whose cost function is

$$J_{LMS} = E [|y(n) - d(n)|^2] \quad (3.1)$$

where $y(n)$ is the equalizer's complex output, $d(n)$ is the ideal or desired signal and $E[\cdot]$ is the expectation operation. However, blind algorithms are different in the formulation of their cost functions. The basic principle is to minimize the error

between the equalizer output and a constant, specified based on the statistics of the transmitted symbol. In this manner, blind equalizers are able to achieve ISI removal without employing any training symbols. This significantly improves the throughput of the system since training data do not carry any useful information. Hence, every transmitted data carries useful information in blind equalization system.

The major problem inherent to blind equalizers is the slow convergence rate of the algorithms since the equalizer output only become useful after the equalizer has converged. Hence, the data transmitted during the converging phase are useless and this can be a significant amount of data in blind equalizers.

The decision to use blind algorithms may be due to cost consideration or might be because they are the only available choice having considered environment realities and system architectures. The use of blind equalizers is found in applications such as Asynchronous Transfer Mode (ATM) Local Area Network (LAN), digital subscriber line (VDSL), Digital Audio and Video Broadcasting, broadband access on copper in Fiber-To-The-Curb (FTTC) and surveillance applications where start-up delay can be tolerated [22–26]. There is a fundamental issue of what should be the nature of signal statistics used for cost functions of blind equalizers. Higher order statistics may provide better performance but they increase the system complexity while second-order statistics seem a good balance between performance and complexity. The major blind equalization algorithms are discussed further in this section.

3.2 Constant Modulus Algorithm (CMA)

CMA is a blind algorithm that is also termed 'Property Restoral' algorithm. It restores the constant envelope of signal lost due to multipath transmission and the resultant ISI. It uses only the signal statistics without employing any trained or pilot symbols thereby improving the throughput and spectral efficiency of the system [27].

CMA [28, 29] basically reduces the error between the magnitude of equalizer output and a circle of constant radius. However, CMA is not able to correct any phase rotation introduced by channel characteristics since its cost function is independent of the phase information hence CMA is said to be "blind to the phase". The complexity of CMA is on the same scale as that of LMS ((3.1)), the most popular trained equalization algorithm. The cost function for CMA is given as

$$J_{\text{CMA}}(n) = E\{|z(n)|^2 - R\}^2 \quad (3.2)$$

where $z(n)$ is the output of the equalizer and R is the Godard dispersion constant [30] defined as

$$R = \frac{E|a(n)|^4}{E|a(n)|^2} \quad (3.3)$$

where $a(n)$ is the transmitted complex-valued data sequence. Denoting equalizer input vector as

$$\mathbf{y}(n) = [y(n), y(n-1), \dots, y(n-N+1)]^T \quad (3.4)$$

and equalizer weight vector as

$$\mathbf{w}(n) = [w_0(n), w_1(n), \dots, w_{N-1}(n)]^T \quad (3.5)$$

for an equalizer of length N , the equalizer output is expressed as

$$z(n) = \mathbf{w}(n)^H \mathbf{y}(n) \quad (3.6)$$

In order to obtain the optimum tap coefficients of the equalizer we use stochastic gradient descent technique to optimize the defined cost function with respect to the equalizer tap coefficients. Therefore, we take stochastic gradient of (3.2) with respect to the tap weights vector to obtain

$$\frac{\partial J_{\text{CMA}}(n)}{\partial \mathbf{w}(n)} = e(n) \mathbf{y}^*(n) \quad (3.7)$$

where $e(n)$ is the error factor and is given as

$$e(n) = 4z(n)(|z(n)|^2 - R) \quad (3.8)$$

and the tap weights vector are recursively updated as

$$\mathbf{w}(n) = \mathbf{w}(n-1) - \mu \mathbf{y}(n) e^*(n) \quad (3.9)$$

Some observations are evident from the expression (3.2) above. First, it is a non-convex function whose shape has been compared to an egg carton as shown in Fig 3.1, possessing stationary points in the form of global maximum, saddle points and local minima [31]. Convergence to these points can be avoided by careful tap initialization of the filter coefficients. Further is its time domain implementation which results in high complexity in channels with long impulse response. Also, a separate carrier phase recovery loop is usually used because CMA seek to only restore the modulus of the received signal and does not perform carrier phase recovery. This inability of CMA to correct the phase of the equalized signal constellation increases the steady-state complexity as adaptive rotator is used in practical applications to correct the phase.

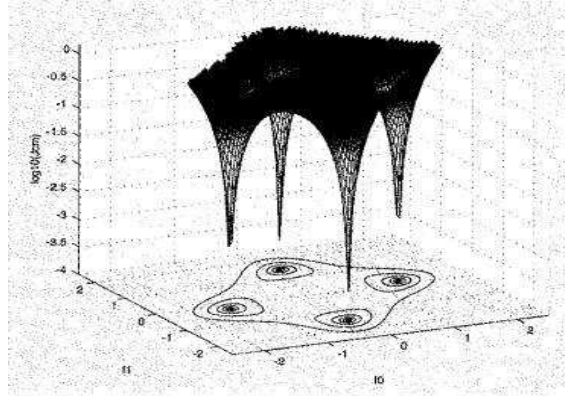


Figure 3.1: CMA cost function surface [30]

3.2.1 Godard dispersion constant

Godard dispersion constant is as computed in (3.3). However, it has a much deeper significance with regards to CMA operation. It can be written as

$$R = r^2 \tag{3.10}$$

where r is called Godard radius. The radius is characteristic of the statistics and the structure of a signal's modulation format. The constant modulus (CM) in CMA is a reference to this radius and for a CM modulation format such as Quadrature Phase-Shift Keying (QPSK), the radius passes through each of the constellation symbols. The constellation of a non-CM signal has different radii but can still be characterized by Godard radius and as such, can be equalized by CMA. This is one of the hidden feature of CMA which is not very clear from cursory observation and it has been demonstrated that CMA can be applied to non-CM signal such as rectangular QAM constellation [28].

3.3 MultiModulus Algorithm (MMA)

MMA addressed the phase ambiguity of CMA by limiting the ambiguity to within $\pm \frac{\pi}{2}$ [12]. MMA, the modified form of CMA, was proposed in [32, 33] to realize a cost function able to perform both blind equalization and carrier phase recovery

simultaneously. The cost function for this algorithm is given as

$$J_{\text{MMA}}(n) = E \left\{ [|z_R(n)|^2 - R_{1,R}]^2 + [|z_I(n)|^2 - R_{1,I}]^2 \right\}, \quad (3.11)$$

where

$$R_{1,R} = \frac{E|a_R(n)|^4}{E|a_R(n)|^2} \quad \text{and} \quad R_{1,I} = \frac{E|a_I(n)|^4}{E|a_I(n)|^2}. \quad (3.12)$$

and both subscript R and I denote real and imaginary parts respectively. However, including both real and imaginary parts of the equalizer output in the cost function and equalizing them separately sometimes results in diagonal solutions [33]. The error sample for MMA can be derived from (3.11) and is given as

$$e(n) = 2 \left[z_R(n) (z_R^2(n) - R_{1,R}) + j z_I(n) (z_I^2(n) - R_{1,I}) \right] \quad (3.13)$$

The decomposition of MMA cost function into real and imaginary parts allow joint blind equalization and phase recovery without the need for a separate rotator or carrier-recovery system as obtained in CMA [34]. In this manner, MMA combines both the benefits of the popular reduced constellation algorithm (RCA) and CMA. RCA has an inherent property to recover the phase in steady state [35] while CMA achieved initial reliable convergence [33].

3.4 Soft Constraint Satisfaction Multimodulus

Algorithm (SCS-MMA)

A new blind algorithm, proposed by Lin [10], was derived by using the dispersion of real and imaginary parts of the MMA equalizer output as constraints and minimizing the squared euclidean norm of the change in the tap-weight vector to ensure that error samples approach zero. The proposed algorithm was based on the principle of minimum disturbance. From Lin algorithm, a new algorithm termed Soft-Constraint Satisfaction Multimodulus Algorithm (SCS-MMA) [9] was derived by relaxing the constraints defined by Lin using principle of soft-constraint satisfaction (SCS) [36, 37]. The cost function for SCS-MMA is given as

$$J_{\text{SCS-MMA}}(n) = E \left\{ \frac{|z_R(n)|^3}{3R_{2,R}} - \frac{z_R^2(n)}{2} + \frac{R_{2,R}^2}{6} + \frac{|z_I(n)|^3}{3R_{2,I}} - \frac{z_I^2(n)}{2} + \frac{R_{2,I}^2}{6} \right\} \quad (3.14)$$

where

$$R_{2,R} = \frac{E[|a_R(n)|^3]}{E[|a_R^2(n)|]} \quad \text{and} \quad R_{2,I} = \frac{E[|a_I(n)|^3]}{E[|a_I^2(n)|]}. \quad (3.15)$$

The error term for SCS-MMA is derived from (3.14) and is given as

$$e(n) = z_R(n) \left(1 - \frac{|z_R(n)|}{R_{2,R}} \right) + j z_I(n) \left(1 - \frac{|z_I(n)|}{R_{2,I}} \right) \quad (3.16)$$

SCS-MMA can also be regarded as a variant of RCA proposed in [38], obtained by removing the discontinuity found in RCA cost function [39]. It is able to recover the phase error of the received signal like RCA and achieve reliable initial conver-

gence as CMA. The technique in [37] applied a constraints to a deterministic cost function in a soft manner by introducing a controlling parameter for controlling the degree of satisfaction. This technique was applied to Lin cost function [10] to soften the control over its convergence speed and realize SCS-MMA [9]. SCS-MMA achieve equalization essentially by forcing the real and imaginary parts of equalizer output onto a four-point contours with distance of R_2 [40].

Blind algorithms as described in this chapter operate on a symbol-by-symbol basis processing a sample at a time. However, in order to take advantage of DFT processing, we need to formulate a block-by-block processing algorithm which will operate on a block of symbols at a time. This approach greatly reduce computational cost, improve efficiency and is the appropriate mode of processing for SC-FDMA equalization.

In the next section, we take advantage of CP embedded in the SC-FDMA block formation in adapting FD blind algorithms to its equalization. It should be noted that the frequency domain processing proposed in this work for SC-FDMA does not require the use of overlap-save and overlap-add convolution techniques because these techniques are needed and employed in order to segment long streams of data for block processing and can be avoided with the inclusion of CP [15]. Additionally, since multiplication in frequency domain for discrete data is essentially circular convolution in time domain, overlap-save and overlap-add techniques help in implementing linear convolution in frequency domain. However, in SC-FDMA case, the received data are in blocks due to the inclusion of CP at the transmitting

Algorithm	Cost Function ($J(n)$)
CMA	$E\{ z(n) ^2 - R\}^2$
MMA	$E\left\{[z_R(n) ^2 - R_{1,R}]^2 + [z_I(n) ^2 - R_{1,I}]^2\right\}$
SCS-MMA	$E\left\{\frac{ z_R(n) ^3}{3R_{2,R}} - \frac{z_R^2(n)}{2} + \frac{R_{2,R}^2}{6} + \frac{ z_I(n) ^3}{3R_{2,I}} - \frac{z_I^2(n)}{2} + \frac{R_{2,I}^2}{6}\right\}$

Table 3.1: Blind Algorithms Cost Functions

Algorithm	Estimation Error ($e(n)$)
CMA	$4z(n)(z(n) ^2 - R)$
MMA	$2[z_R(n)(z_R^2(n) - R_{1,R}) + jz_I(n)(z_I^2(n) - R_{1,I})]$
SCS-MMA	$z_R(n)\left(1 - \frac{ z_R(n) }{R_{2,R}}\right) + jz_I(n)\left(1 - \frac{ z_I(n) }{R_{2,I}}\right)$

Table 3.2: Blind Algorithms Estimation Errors

end. It is this block of data, kept from interblock interference (IBI) due to the appended CP, that are fed into the equalizer for FD equalization.

3.5 Summary

This chapter summarized the main blind algorithms considered in this work. These algorithms are CMA, MMA and SCS-MMA. Table 3.1 and 3.2 give a synopsis of the algorithms' cost functions and estimation errors.

CHAPTER 4

FREQUENCY DOMAIN BLIND ALGORITHMS

4.1 Introduction to FD Implementation

The early effort in the field of equalization development focused solely on time domain implementation of algorithms and their improvements. However, as data rate increases, the dispersive effect of transmitting medium become more pronounced and receiver design had to be modified to cater for this new development. Time domain equalization, with time, became unsuitable for channels such as broadband wireless transmitting medium with long impulse response and large delay spread. This is due to the prohibitive computational complexity accompanying such implementation because neutralizing the effects of a large dispersion required long equalizers with high number of tap coefficients resulting in high computational cost per symbol [41]. Frequency domain equalization provides a means of

drastically reducing this computational requirement with increasing data rate.

Frequency domain processing was brought into fore by the discovery that FFT could reduce the complexity of FD equalization of block of signal samples [42, 43] followed by the development of overlap-save and overlap-add FD implementation techniques [44]. As a result of the aforementioned reasons, frequency domain (FD) implementation of blind algorithms became highly desired. FD implementation not only reduces computational complexity by performing block-based processing, it also offers faster convergence, achieve lower MSE and several other advantages [11]. There have been many reported superior performance of FD implementation of blind algorithms in the literature.

The most popular blind algorithm, constant modulus algorithm (CMA) was implemented in frequency domain by [41], [45] and [46]. Also, frequency domain implementation of modified CMA (MCMA) was presented in [12] where it was shown that as equalizer length increases, the performance of frequency domain equalizer improves making it suitable to equalization of channels with long impulse response. More recently, frequency domain square contour algorithm (FD-SCA) was proposed in [47]. FDSCA was shown to achieve similar performance with SCA but required significantly less computations for the same filter length. This chapter presents a frequency domain implementation of the soft-constraint satisfaction multimodulus algorithm (FDSCS-MMA). This algorithm was derived by applying the principle of soft-constraint satisfaction to relax the constraints in Lin's cost function [10]. The superior performance of SCS-MMA over Lin's cost

function was shown in [9]. The FD implementation greatly reduces computational complexity associated with time domain implementation of SCS-MMA. Furthermore, performance is greatly improved by proposing a normalized version of the FDSCS-MMA. Normalized FDSCS-MMA shows great performance improvement over SCS-MMA in terms of faster convergence rate of MSE and ISI curves, smaller residual MSE with similar BER performance.

Frequency domain implementation of blind equalizers brings about an issue on whether the error factor is computed in time or frequency domain. The error can be computed on a sample-by-sample basis for each block sample and then transformed to frequency domain or the desired response (signal statistics in blind equalization) can be transformed into frequency domain where the error is computed on a block -by-block basis in frequency domain. However, the frequency domain error computation is the same as time-domain computation for those algorithms where the error is a linear function of the signal like LMS because DFT is a linear operator and the error computation commutes in both domain [48,49]. This is not the case for blind equalization algorithms as their error is a non-linear-function of the signal and the two operations do not commute hence, error is computed in time domain then transform to frequency domain.

The frequency domain implementation considered in this work has been done in two phases. Time domain SCS-MMA algorithm has been compared to the proposed frequency domain SCS-MMA (FDSCS-MMA) in terms of computational complexity and performance. Overlap-save convolution technique was used in

order to carry out this comparative analysis since multiplication in frequency domain for discrete data is essentially circular convolution in time domain. Hence, in the first phase, linear convolution has been achieved in frequency domain through the use of overlap-save convolution technique. In the second phase, cyclic-prefixed single carrier system (CPSCS) results in periodic transmitted symbols which trick the channel to perform circular convolution rather than linear convolution. The periodicity is then removed at the receiver before carrying out frequency domain equalization. This sort of transmission format eliminates the need for overlap-save convolution method since the received signal is a product of circular convolution between the channels and transmitted symbols. Therefore, we simply feed the received symbol into the equalizer. It is the overlap-save convolution technique which is ubiquitous in the literature in implementations such as [12], [47] and [49] that is considered in this chapter. Frequency domain blind adaptive equalization for SC-FDMA, considered in the next chapter, is a relatively new area.

4.2 Overlap-Save Convolution Method

There are two major operations involved in time domain equalization detailed in chapter (3). They are linear convolution embodied by the filtering operation in (3.6) and linear correlation in the update equation of (3.9). In this section, we take advantage of DFT processing in implementing these two operations which leads to circular correlation and circular convolution respectively. In order to implement frequency domain equalization for a long stream of received data, overlap-save

technique is usually employed [50]. This is due to the fact that multiplication in frequency domain (DFT processing) is equivalent to circular convolution in time domain hence, overlap sectioning method is implemented. Similar treatment of other blind algorithms can be found in the literature [12, 47, 49]. The equalizer input is a block of data realized by overlapping its samples. A block size N is defined, usually N is a power of 2 to ensure efficient DFT processing, and equalizer input are divided into blocks of $2N$ consisting of N samples each from previous and current block. In this case, a $2N \times 1$ equalizer block input is defined as

$$\tilde{\mathbf{x}}_k = [x(kN - N + 1), \dots, x(KN), x(KN + 1), \dots, x(kN + N)]^T \quad (4.1)$$

and $2N \times 1$ equalizer weight vector, formed by appending N zeros, is

$$\tilde{\mathbf{w}}_k = [w(0), \dots, w(N - 1), 0, \dots, 0]^T \quad (4.2)$$

The DFT of (4.1) and (4.2) respectively yield

$$\tilde{\mathbf{X}}_k = \mathbf{F}\tilde{\mathbf{x}}_k \quad (4.3)$$

and

$$\tilde{\mathbf{W}}_k = \mathbf{F}\tilde{\mathbf{w}}_k \quad (4.4)$$

\mathbf{F} is a $2N \times 2N$ DFT matrix defined as

$$\mathbf{F} = \left(\frac{1}{\sqrt{2N}} e^{-i \frac{2\pi}{2N} jk} \right)_{j,k=0,\dots,2N-1} \quad (4.5)$$

The $\frac{1}{\sqrt{2N}}$ is a normalization factor to ensure the same signal output power. Hence, the k th block of the equalizer output can be implemented with IDFT as

$$\tilde{\mathbf{z}}_k = \mathbf{D}\mathbf{F}^H(\tilde{\mathbf{X}}_k \odot \tilde{\mathbf{W}}_k) \quad (4.6)$$

where

$$\tilde{\mathbf{z}}_k = [z(0), z(1), \dots, z(N-1)]^T \quad (4.7)$$

and \odot is the element-wise multiplication while matrix \mathbf{D} defined as

$$\mathbf{D} = \begin{bmatrix} \mathbf{0}_N & \mathbf{I}_N \end{bmatrix} \quad (4.8)$$

is used in discarding the upper N components. \mathbf{I}_N denotes $N \times N$ identity matrix and $\mathbf{0}_N$ denotes $N \times N$ zero matrix. Using equalizer output, each element of the error factor can be computed as

$$\tilde{\mathbf{e}}_k(n) = \tilde{\mathbf{z}}_{k,R}(n) \left(1 - \frac{|\tilde{\mathbf{z}}_{k,R}(n)|}{R_{2,R}} \right) + j\tilde{\mathbf{z}}_{k,I}(n) \left(1 - \frac{|\tilde{\mathbf{z}}_{k,I}(n)|}{R_{2,I}} \right) \quad (4.9)$$

and the error factor is

$$\tilde{\mathbf{e}}_k = [e(0), e(1), \dots, e(N-1)]^T \quad (4.10)$$

The error factor is then prepended with N zeros and DFT is taken as

$$\tilde{\mathbf{E}}_k = \mathbf{F}[\mathbf{0}_{N \times 1}; \tilde{\mathbf{e}}_k] \quad (4.11)$$

where $\mathbf{0}_{N \times 1}$ is an $N \times 1$ zero vector. An important observation is noted in (4.9) where the error factor is being computed in time domain. It is stated earlier that only correlation and convolution operations, which correspond to computation of equalizer output and weight update respectively, are carried out in frequency domain. This is because error functions of blind equalizers are non-linear and their frequency domain implementation is not equivalent to their time domain implementation hence, the transform is done in (4.11). The weight update recursion of (3.9) is then implemented with DFT as

$$\tilde{\mathbf{W}}_{k+1} = \tilde{\mathbf{W}}_k + \mu \mathbf{F} \mathbf{G} \mathbf{F}^H (\tilde{\mathbf{X}}_k^* \odot \tilde{\mathbf{E}}_k) \quad (4.12)$$

where

$$\mathbf{G} = \begin{bmatrix} \mathbf{I}_N & \mathbf{0}_N \\ \mathbf{0}_N & \mathbf{0}_N \end{bmatrix} \quad (4.13)$$

Both (4.6) and (4.12) completely describe the equalizer operation in frequency domain.

$\mathbf{F} \mathbf{G} \mathbf{F}^H$ in (4.12) is used to implement gradient constraint. Implementation of gradient constraint increases complexity but results in lower residual MSE. We find

that the convergence of FDSCS-MMA can be improved greatly by considering the square root of the spectral power of the equalizer input as a normalization factor and the improved algorithm is subsequently referred to as normalized frequency domain SCS-MMA (NFDSCS-MMA). Therefore, each frequency bin in the weight update equation is normalized by square root of the spectral power of its respective input data. Both the power recursion used for normalization and the resulting normalized weight update equation are, respectively, given by

$$\boldsymbol{\alpha}_k(n) = \beta \boldsymbol{\alpha}_{k-1}(n) + (1 - \beta) |\tilde{\mathbf{X}}_k(n)|^2 \quad (4.14)$$

$$\tilde{\mathbf{W}}_{k+1} = \tilde{\mathbf{W}}_k + \mu \mathbf{G}(\tilde{\mathbf{X}}_k^* \odot \tilde{\mathbf{E}}_k \oslash \sqrt{\boldsymbol{\alpha}_k}) \quad (4.15)$$

where

$$\boldsymbol{\alpha}_k = [\alpha(0), \alpha(1), \dots, \alpha(N-1)]^T \quad (4.16)$$

β is a forgetting factor in (4.14) and \oslash in (4.15) is an element-wise division operator. A careful re-ordering of the normalized weight update equation reveal another insightful observation into its effectiveness in improving the equalizer convergence. It is seen that the normalization is tantamount to using variable step size in each of the frequency bins which amounts to power control on each bin and such technique is especially useful in applications where the input level is uncertain or vary widely across the band as noted in [11]. The structure of the proposed NFDSCS-MMA using overlap-save technique is depicted in Fig. 4.1

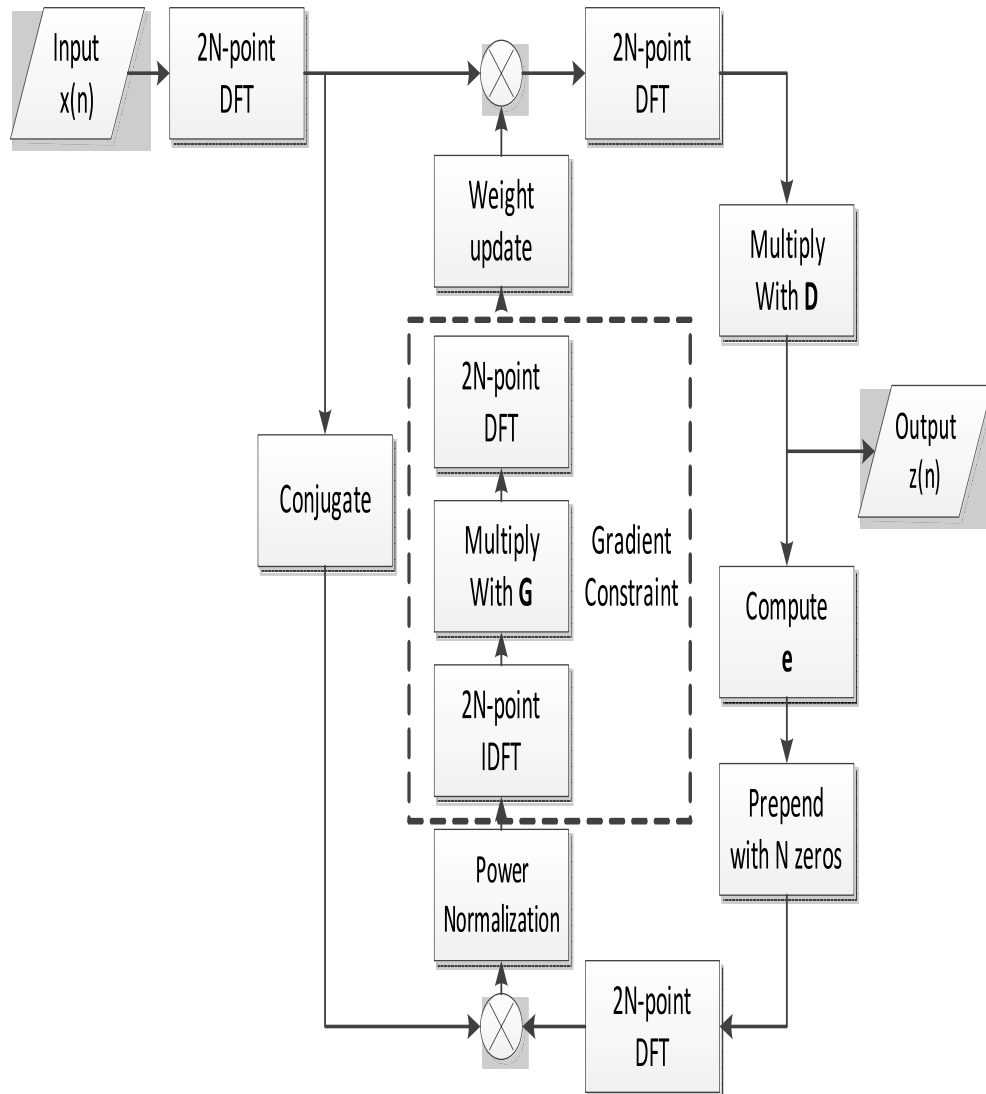


Figure 4.1: Normalized NFDSCS-MMA equalizer with overlap-save method.

4.3 Computational Complexity

There are basically 3 operations involved in the equalization process. They are filtering operation (which results in the equalizer output), error calculation and weight update. The real multiplications involved in carrying out these operations is calculated here in order to assess and compare the computational complexity of the algorithms.

The filtering operation of (3.6) involve N complex multiplications which requires to $4N$ real multiplications due to the fact that one complex multiplication requires four real multiplications [51]. Error calculation of (3.16) requires 4 real multiplications. Further, the weight update in (3.9) requires N complex multiplications for the evaluation of $e(n)y^*(n)$ and an additional $2N$ real multiplications to account for μ evaluation in the update equation.

Hence, in total, the real multiplications required per input symbol in an equalizer of length N using SCS-MMA algorithm is

$$\mathcal{O}_{\text{SCS}} = 10N + 4 \quad (4.17)$$

The required number of real multiplications for an N -point FFT/IFFT is $2N \log_2(N)$ [52]. A $2N$ -point FFT is required to obtain $\tilde{\mathbf{X}}_k$ and $\tilde{\mathbf{E}}_k$ while a $2N$ -point IFFT is required for obtaining $\tilde{\mathbf{z}}_k$ with additional $2N$ complex multiplications for obtaining frequency domain equalizer output. Calculation of error factor in (4.10) and multiplication with μ in the weight update equation each

Table 4.1: Number of Real Multiplications for Varying Equalizer Length

N	TD	FD	NFD	$\mathcal{O}_{\text{NFD}}/\mathcal{O}_{\text{TD}}$
2	24	64	72	308.33%
4	44	84	92	209.10%
8	84	104	112	133.33%
16	164	124	132	80.49%
32	324	144	152	46.91%
64	644	164	172	26.71%
128	1284	184	192	14.95%
256	2564	204	212	8.27%

require N complex multiplications. $2N$ complex multiplications are each required for the evaluation of $\tilde{\mathbf{X}}_k^* \odot \tilde{\mathbf{E}}_k$ and the subsequent element-wise division in the normalized equation of (4.15). Finally, the gradient constraint requires a $2N$ – point FFT/IFFT pair. Therefore, the total required number of real multiplications for evaluating NFDSCS-MMA is

$$\mathcal{O}_{\text{NFD}} = 20N \log_2(2N) + 32N \quad (4.18)$$

The equivalent real multiplications per symbol is then

$$\mathcal{O}_{\text{NFD}} = 20 \log_2(2N) + 32 \quad (4.19)$$

It should be noted that the equation in (4.12) requires 8 real multiplications less than that required for equation (4.15). Table 4.1 and Fig. 4.2 show the computational complexity between SCS-MMA, FDSCS-MMA and NFDSCS-MMA for different lengths of the equalizer.

Figure 4.2 shows that as the length of the equalizer increases, complexity

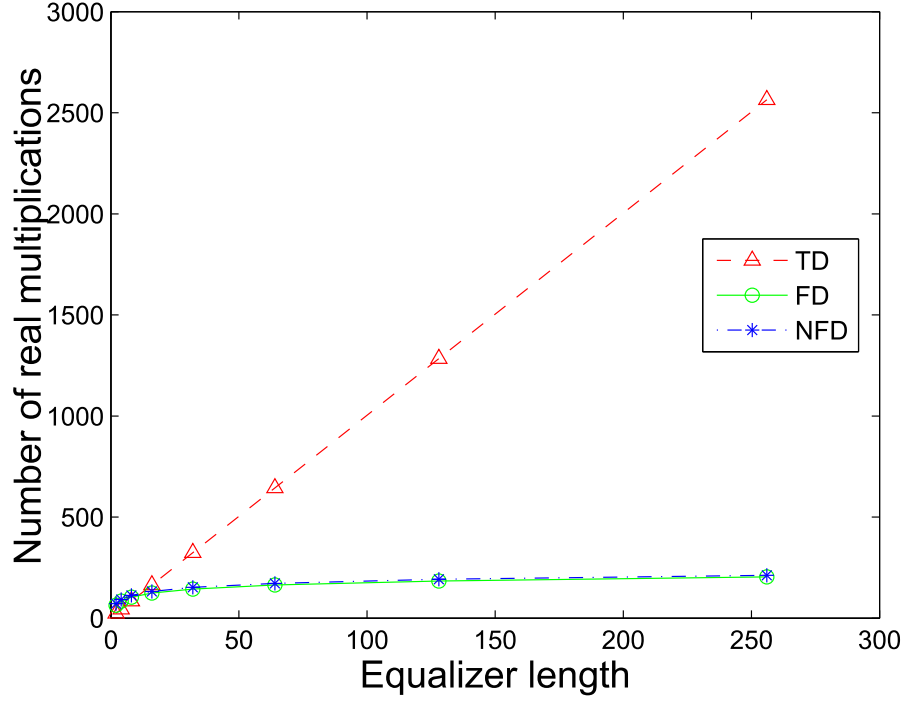


Figure 4.2: Comparison of computational complexity for varying length of equalizer.

increases logarithmically for NFDSCS-MMA and FDSCS-MMA but increases linearly for SCS-MMA such that only 8.27% of the computational complexity of SCS-MMA is required for NFDSCS-MMA for equalizer length $N = 256$. This shows the huge computational savings realized from implementation of NFDSCS-MMA especially for long equalizer length.

4.4 Performance Measures

The performance of the equalization algorithms developed in this work were accessed using the four major performance criteria . The criteria are detailed below.

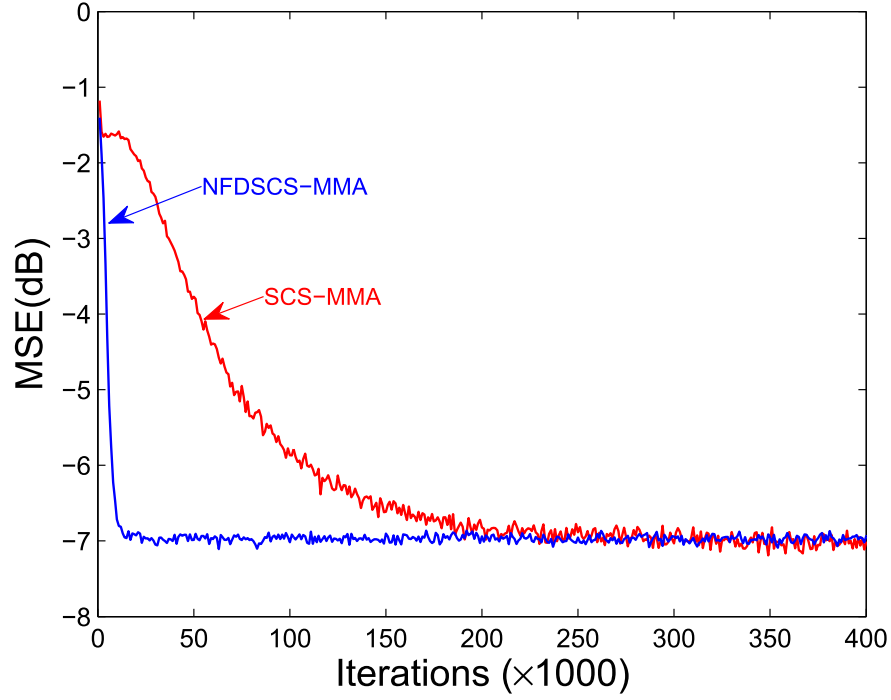


Figure 4.3: MSE convergence comparison for equalizer length $N = 64$, SNR=10dB.

4.4.1 Mean Square Error (MSE)

Mean Square Error is the evaluation of the average of the squares of the errors made by the algorithm. It essentially measures how far the equalizer output is from the cost function objective. MSE for blind equalizers is plotted with regard to their cost functions. Table 3.1 and 3.2 provide a summary of the blind equalization algorithms considered in this work. The lower the residual MSE, the better the algorithm achieved its minimization objective.

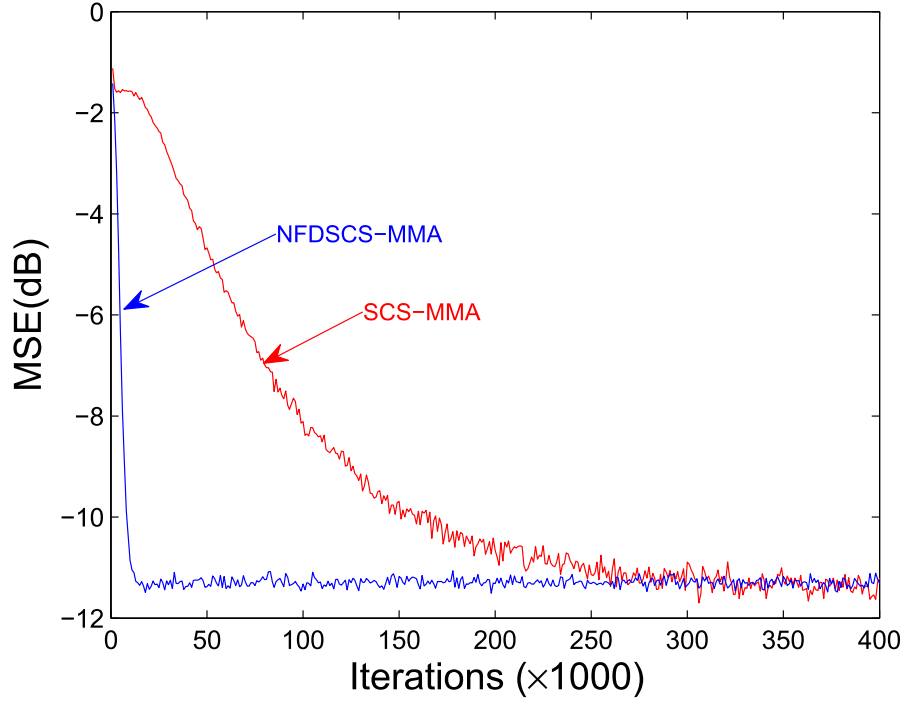


Figure 4.4: MSE convergence comparison for equalizer length $N = 64$, SNR=20dB.

4.4.2 Inter-symbol Interference (ISI)

The residual ISI at the output of the equalizer at n th iteration is given as [53]

$$ISI(n) = \frac{\sum |s(n)|^2 - |s(n)|_{max}^2}{|s(n)|_{max}^2} \quad (4.20)$$

where $|s(n)|$ is the overall impulse response of the transmission channel ($h(n)$) and equalizer ($w(n)$). $|s(n)|_{max}$ is the component with maximum absolute value among all the components of $|s(n)|$ and $[*]$ denotes convolution. ISI indicates the effectiveness of the algorithm to remove the channel-introduced ISI and is the true metric of blind equalizers.

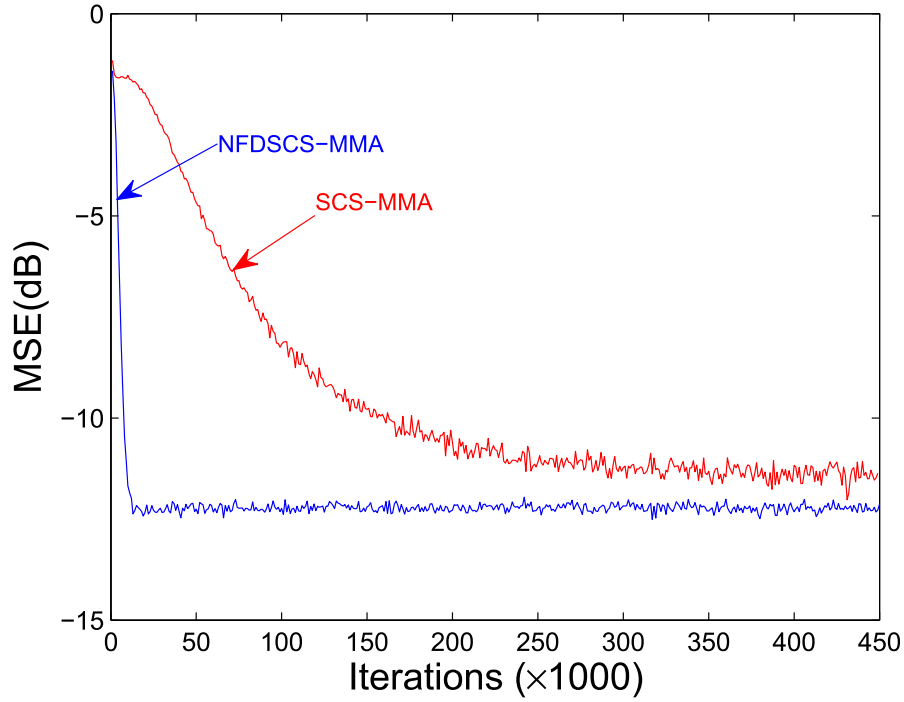


Figure 4.5: MSE convergence comparison for equalizer length $N = 64$, SNR=30dB.

4.4.3 Symbol Constellation

This indicate the effectiveness of the algorithm to restore the constellation of the transmitted symbols after it has been distorted by the channel characteristics. It indicates the open-eye ability of the algorithm.

4.4.4 Bit Error Rate

This measures the rate at which error occurs in a system. It can be defined as the ratio of number of error bits to the total number of transmitted bits. It is an important criteria used in the assessment of digital transmission system. The factors that affect BER include ISI, transmitter power, modulation technique and

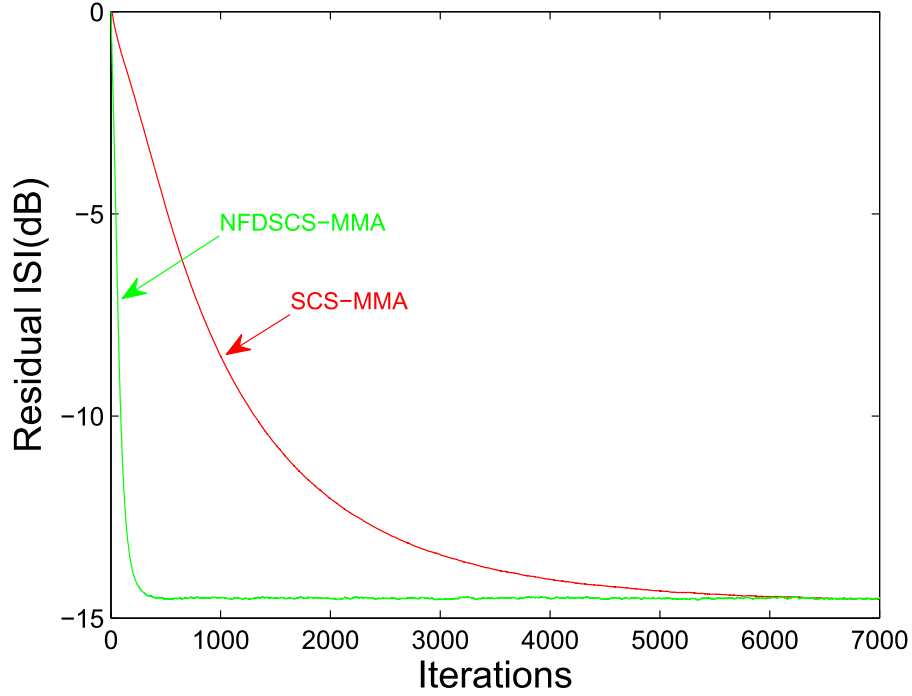


Figure 4.6: Residual ISI convergence curves for equalizer length $N = 64$, SNR=10dB.

available bandwidth.

4.5 Simulation Results

The performance of the proposed algorithms were investigated by means of computer simulations in MATLAB environment. Specifically, we have evaluated the performance of normalized FDSCS-MMA , FDSCS-MMA and SCS-MMA and compared the results. A 4-QAM data set is used with a Vehicular A channel [3]. The step size for the equalizers are 1×10^{-2} , 7×10^{-4} and 1.3×10^{-3} for NFDSCS-MMA, FDSCS-MMA and SCS-MMA respectively while β is 0.955.

Figure 4.3, Figure 4.4 and Figure 4.5 show the MSE performance of the equal-

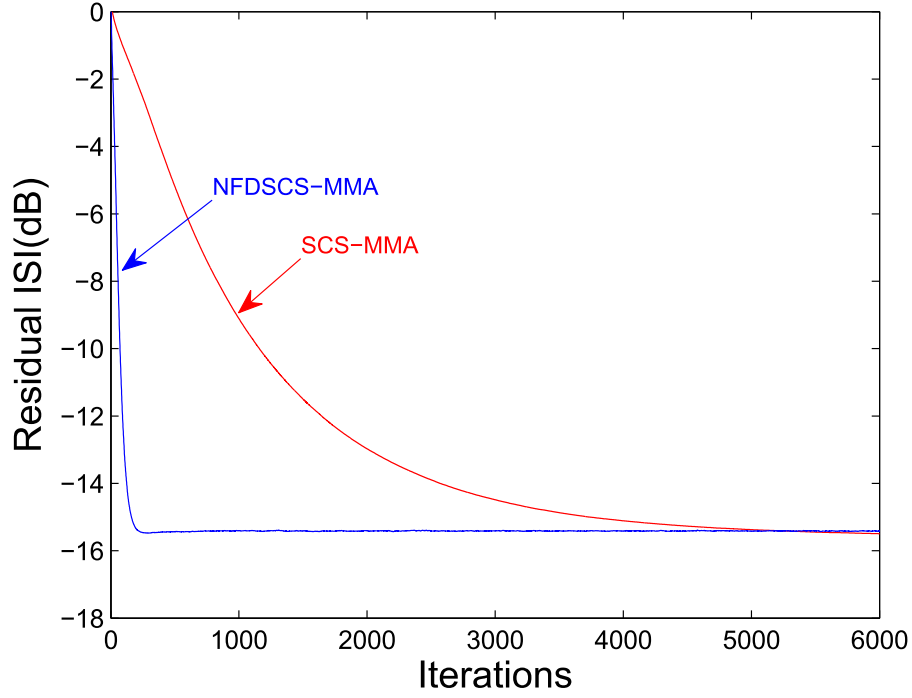


Figure 4.7: Residual ISI convergence curves for equalizer length $N = 64$, SNR=20dB.

izer at different SNRs for the same equalizer length of $N=64$. Different SNRs are considered in order to evaluate the equalizer performance under different conditions. It is observed that for a fixed length of the equalizer ($N=64$), MSE convergence rate become slower as SNR increases from 10dB to 30dB for SCS-MMA while it stays the same for NFDSCS-MMA. Also the residual MSE is smaller for NFDSCS-MMA at high SNR of 30dB but stays the same as that of SCS-MMA at lower SNRs. The speed of MSE convergence is faster for NFDSCS-MMA compared to SCS-MMA, for all SNR scenarios considered, which show that the normalized FD implementation is better.

Figure 4.6, Figure 4.7 and Figure 4.8 show the ISI performance of the equalizer at different SNRs for the same equalizer length of $N=64$. NFDSCS-MMA has the

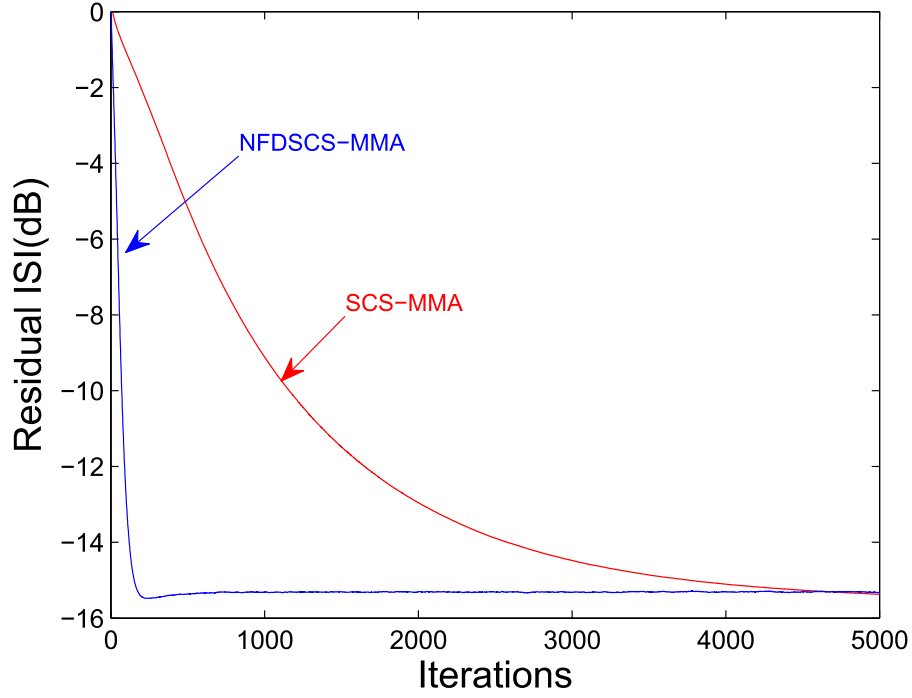


Figure 4.8: Residual ISI convergence curves for equalizer length $N = 64$, SNR=30dB.

same residual ISI compared to SCS-MMA for all the SNR scenarios but converges faster in each scenario. This shows that NFDSCS-MMA is able to suppress the channel-introduced ISI faster than SCS-MMA which makes it better and more suited to high-speed broadband wireless transmission.

Figure 4.9 shows MSE performance of the equalizers for $N=128$ and SNR of 20dB. It is seen that SCS-MMA has the highest residual MSE but converges faster than FDSCS-MMA. However, NFDSCS-MMA has the fastest convergence and outperformed SCS-MMA in both rate of convergence and residual MSE. This performance improvement is an indication of the effectiveness of the normalization factor.

Figure 4.10 shows MSE performance for long equalizer of length $N=256$. It

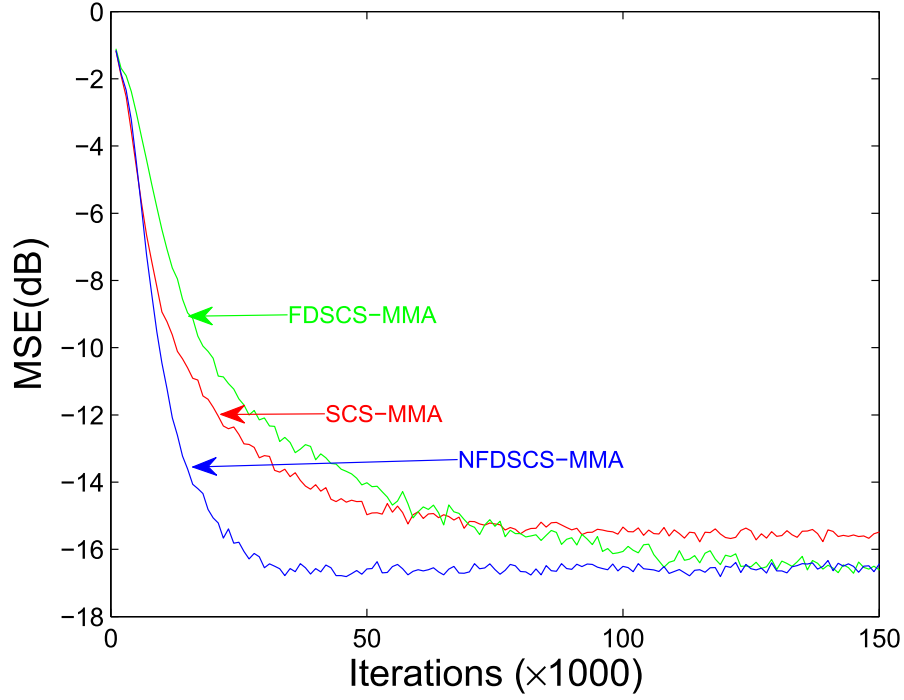


Figure 4.9: MSE convergence comparison for equalizer length $N = 128$.

is seen that the proposed algorithm converges fastest and has the least residual MSE. It converges about 2 times faster and has a gain of more than 3dB in residual MSE. This confirms the suitability of the proposed equalizer to channels requiring long equalizer length such as broadband wireless systems.

Figure 4.11 and Figure 4.12 show the corresponding residual ISI for $N=128$ and 256. It is seen that NFDSCS-MMMA has better performance as it achieves faster convergence than both FDSCS-MMA and SCS-MMA.

Finally, Figure ?? shows that both NFDSCS-MMA and SCS-MMA has similar BER performance. This indicates no loss of performance by the proposed algorithm despite the huge savings in computational complexity and resulting adaptation to broadband wireless systems.

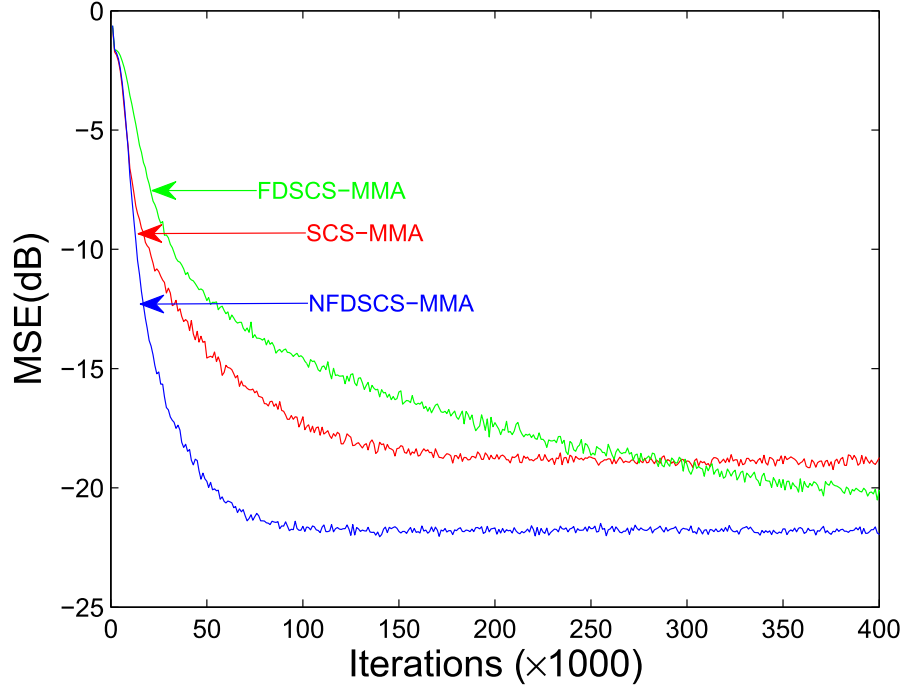


Figure 4.10: MSE convergence comparison for equalizer length $N = 256$.

4.6 Summary

In this section, a frequency domain implementation of the SCS-MMA (FDSCS-MMA) has been proposed. The frequency domain implementation greatly reduces computational complexity encountered in the time domain implementation. Performance of FDSCS-MMA is improved by considering an appropriate normalization factor. The normalized FDSCS-MMA outperformed both SCS-MMA and FDSCS-MMA in both convergence rate and residual MSE especially for long equalizer. This superior performance is noted for all the SNR scenarios (low to high SNR) considered. Hence, this shows that NFDSCS-MMA is well suited to broadband wireless systems, characterized with long channel impulse response and large delay spread, due to its low computational complexity, faster convergence

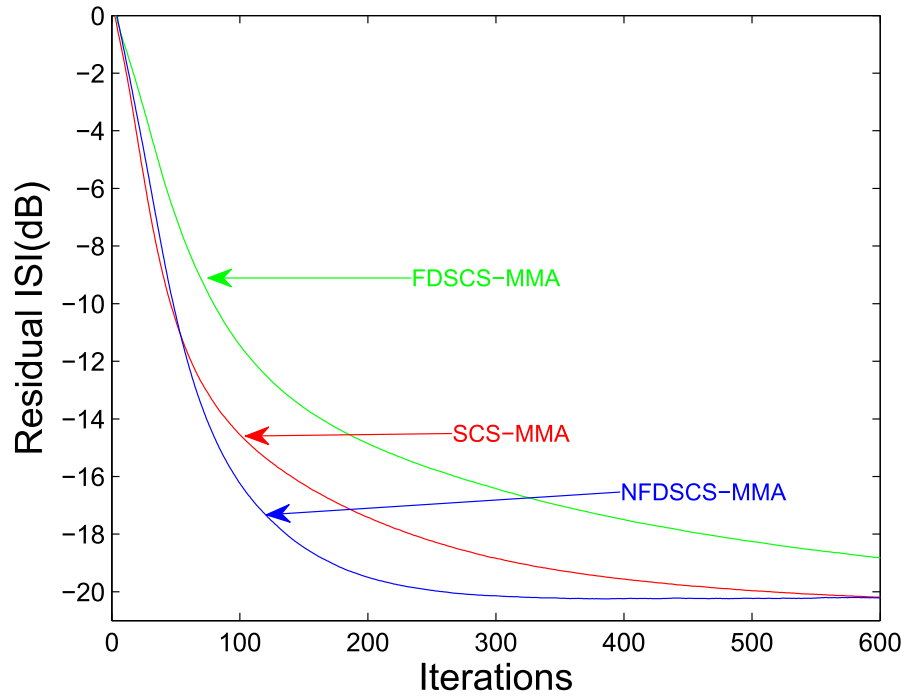


Figure 4.11: Residual ISI convergence curves for equalizer length $N = 128$.

rate, lower residual MSE and comparable BER performance.

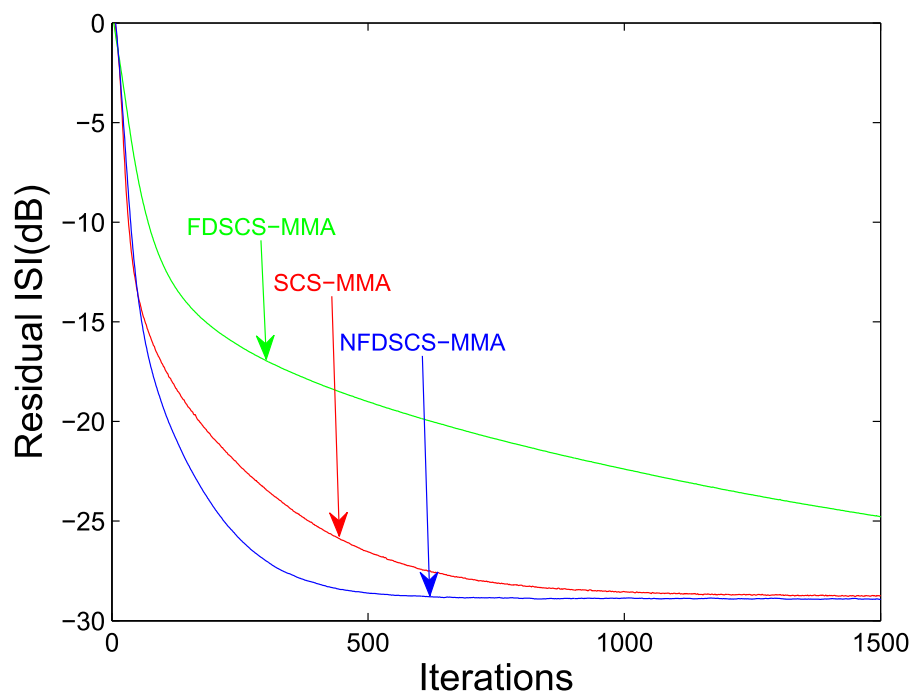


Figure 4.12: Residual ISI convergence curves for equalizer length $N = 256$.

CHAPTER 5

FDSCS-MMA FOR SCFDMA

5.1 Introduction to FDBE-SC-FDMA

Frequency domain blind equalization of SC-FDMA (FDBE-SC-FDMA) is developed and implemented in this chapter. It has been shown in Chapter 4 that the frequency domain implementation of SCS-MMA outperformed time-domain SCS-MMA in terms of complexity, convergence rate, residual MSE and that as a result, NFDSCS-MMA is specially suited to broadband wireless systems characterized by long impulse response and large delay spread. Also, due to the 14% throughput degradation in uplink SC-FDMA, NFDSCS-MMA serves as an attractive solution. Its application to SC-FDMA equalization removes the throughput degradation as it does not use training symbols in its equalization approach. In this chapter, NFDSCS-MMA is adapted to equalize SC-FDMA with resultant significant improvement in throughput and spectral efficiency.

It was mentioned in Chapter 4 that the special nature of SC-FDMA which include

DFT processing and insertion of CP at the transmitter ensures that the received data is in blocks rather than long streams which implies that we do not require the use of overlap-save or overlap-add sectioning method.

5.2 NFDSCS-MMA without Overlap-Save Technique

The block diagram of the equalizer is presented in Fig. 5.1 for a single user. The DFT of tap weight vector for kth received block will yield

$$\mathbf{W}_k = \mathbf{F}_N \mathbf{w}_k \quad (5.1)$$

where

$$\mathbf{w}_k = [w(0), \dots, w(N-1)]^T \quad (5.2)$$

Hence, the kth block of the equalizer output can be implemented with DFT as

$$\mathbf{z}_k = \mathbf{F}_N^H (\mathbf{Y}_k \odot \mathbf{W}_k) \quad (5.3)$$

where

$$\mathbf{z}_k = [z(0), z(1), \dots, z(N-1)]^T \quad (5.4)$$

and \odot is the element-wise multiplication while \mathbf{Y} is as defined in Chapter 2. Using the equalizer output, the error factor can be computed and its DFT taken as

$$\mathbf{E}_k = \mathbf{F}_N \mathbf{e}_k \quad (5.5)$$

where

$$\mathbf{e}_k = [e(0), e(1), \dots, e(N-1)]^T \quad (5.6)$$

and

$$\mathbf{e}_k(n) = \mathbf{z}_{k,R}(n) \left(1 - \frac{|\mathbf{z}_{k,R}(n)|}{R_{2,R}}\right) + j\mathbf{z}_{k,I}(n) \left(1 - \frac{|\mathbf{z}_{k,I}(n)|}{R_{2,I}}\right) \quad (5.7)$$

The weight update recursion is then implemented with DFT as

$$\mathbf{W}_{k+1} = \mathbf{W}_k + \mu(\mathbf{Y}_k^* \odot \mathbf{E}_k) \quad (5.8)$$

Both (5.3) and (5.8) completely characterize the equalizer operation in frequency domain.

The error functions of equalizers are derived from their cost functions and this cost functions are different for different equalizers. Table 3.1 and 3.2 give a synopsis of blind algorithm cost functions and error functions respectively. Following the preceding discussion, both CMA and MMA can easily be fitted into the developed framework by substituting their respective error factors. We find that the convergence of SCS-MMA can be greatly improved, as implemented in Chapter 4, by considering the square root of the spectral power as a normalization factor

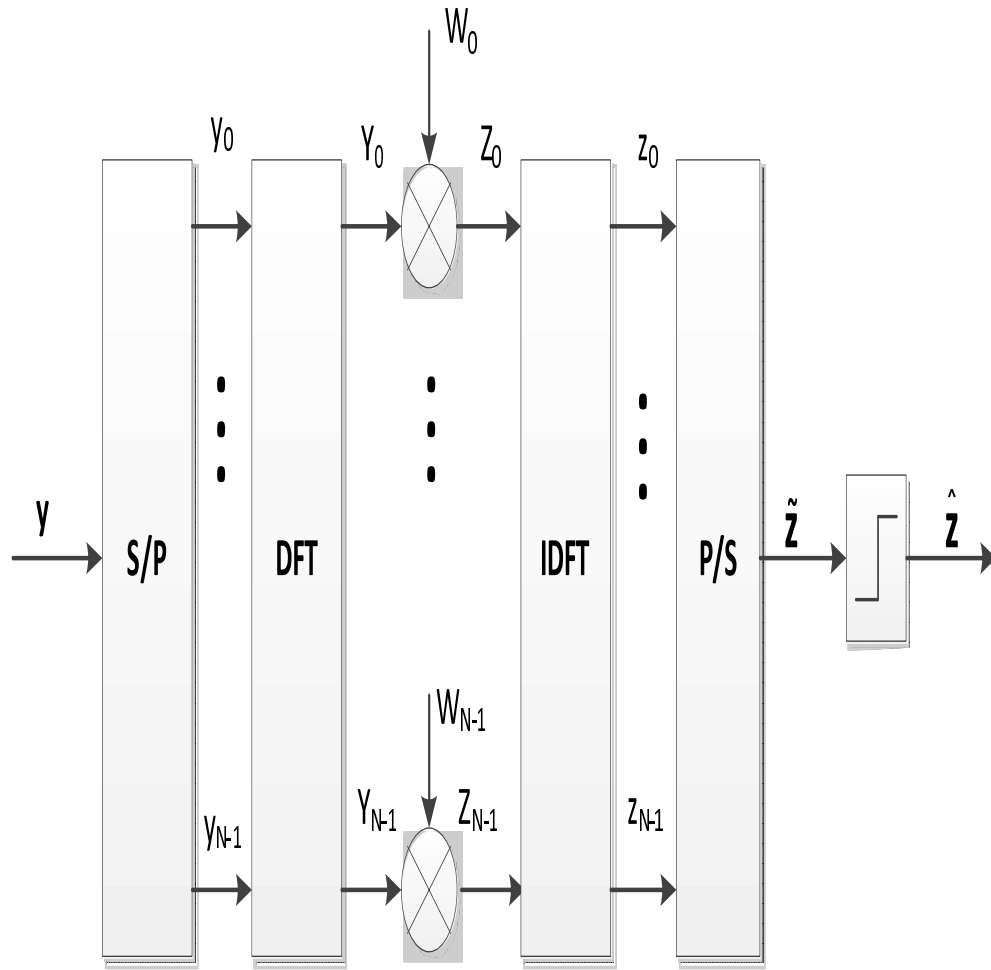


Figure 5.1: Block diagram of FD equalizer.

and we subsequently referred to the improved algorithm as normalized frequency domain SCS-MMA (NFDSCS-MMA). Therefore, each frequency bin in the weight update equation of (5.8) is normalized by the spectral power of its respective input data. Both the power recursion and resulting normalized weight update equation are given by (5.9) and (5.10) respectively.

$$\mathbf{P}_k(n) = \lambda \mathbf{P}_{k-1}(n) + (1 - \lambda) |\mathbf{Y}_k(n)|^2 \quad (5.9)$$

$$\mathbf{W}_{k+1} = \mathbf{W}_k + \mu (\mathbf{Y}_k^* \odot \mathbf{E}_k \oslash \sqrt{\mathbf{P}_k}) \quad (5.10)$$

where

$$\mathbf{P}_k = [P(0), P(1), \dots, P(N-1)]^T \quad (5.11)$$

λ is a forgetting factor in (5.9) and \oslash in (5.10) is an element-wise division operator. The procedure outlined in this section is repeated to realize normalized FDMMA (NFDMMMA) and normalized FDCMA (NFDCCMA) from the equations given in Table 3.1 and 3.2 and the details of the algorithm is given in Fig. 5.2.

5.3 Simulation results

5.3.1 Experiment 1

Specifically, we have evaluated the performance of NFDMMMA, FDMMA, NFDCCMA and FDCMA for both IFDMA and LFDMA. In order to simulate multi-user environment, we use transmitter FFT size of 256 equivalent to the total available

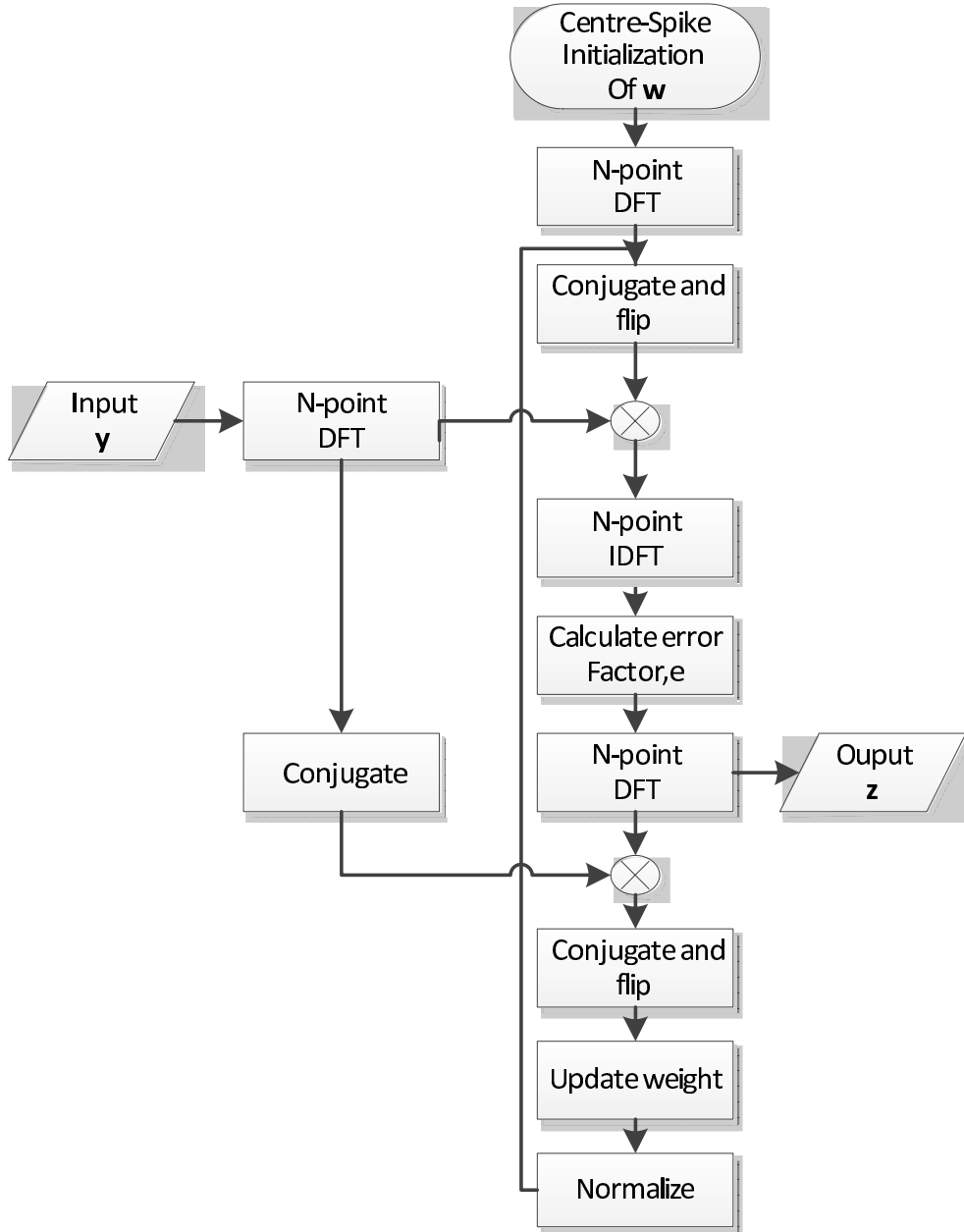


Figure 5.2: Normalized FDSCS-MMA algorithm.

subcarriers in the system (M), input FFT size for a user is 64 same as the number of subcarriers available for each user (N) and length of CP is 20 samples (P). This makes a total number of 4 users whose data were transmitted simultaneously.

Mean square error (MSE) convergence curve in dB was obtained as ensemble average and is plotted as a function of the number of iterations where each iteration represent an SC-FDMA symbol consisting of all the users' signal for that transmission. The filter taps are of the order of N with center-spike initialization. Quadrature phase shift keying (QPSK) modulation was employed for MSE plot.

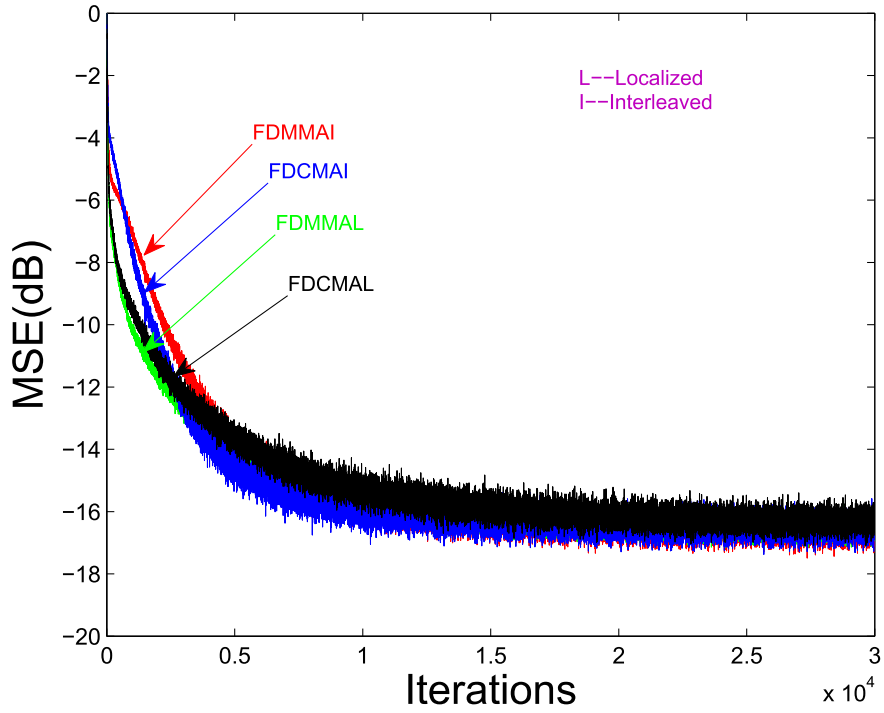


Figure 5.3: MSE curves for unnormalized FD blind algorithms.

The values of R , $R_{2,R}$, $R_{2,I}$ and λ are 1, 1/2, 1/2 and 0.55 respectively. The step size for the equalizers are 8×10^{-4} , 2×10^{-4} , 2×10^{-5} and 8×10^{-6} for NFD-MMA, NFDCMA, FDMMA and FDCMA respectively. The channel considered

is Rayleigh fading with 6 taps, each fading independently. Vehicular speed of 1×10^{-4} is used to account for time variation in the channel. The additive white Gaussian noise have been chosen such that the signal to noise ratio at the input of the equalizer varies from 10dB to 30dB in order to assess the performance of the equalizers for different SNR scenarios.

Figure 5.3 shows the performance of FDCMA and FDMMA for both IFDMA and LFDMA. It is seen that the equalizers took a long time to converge, about 20,000 symbols, which is typical of blind algorithms. This slow adaptation is a setback in broadband wireless communication system which typically require high speed transmission.

Figure 5.4 shows performance of NFDMMMA and NFDCMA for IFDMA and

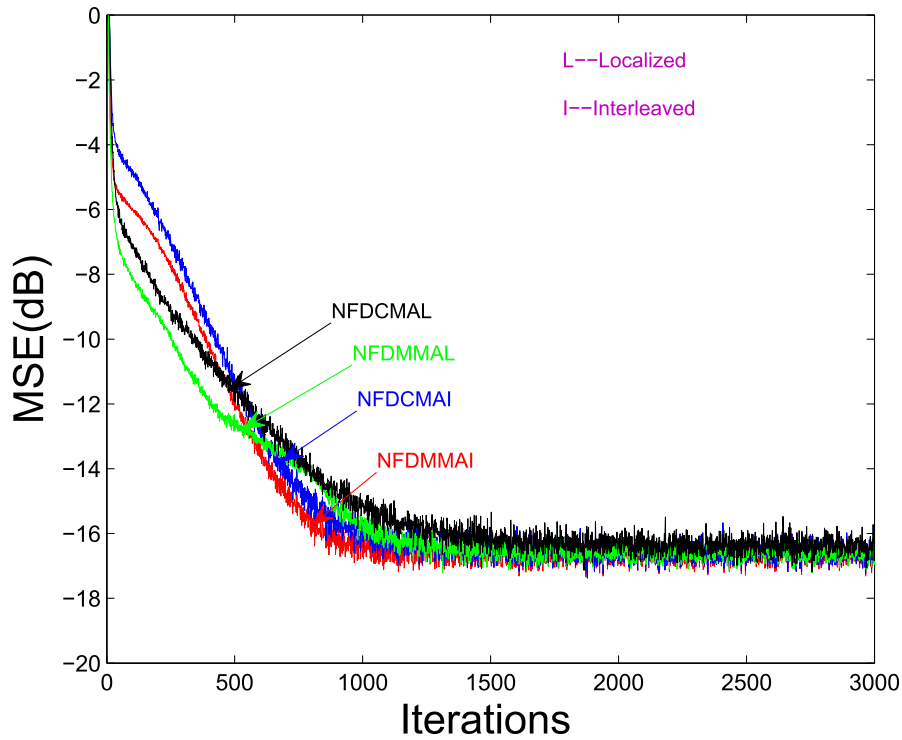


Figure 5.4: MSE curves for normalized FD blind algorithms.

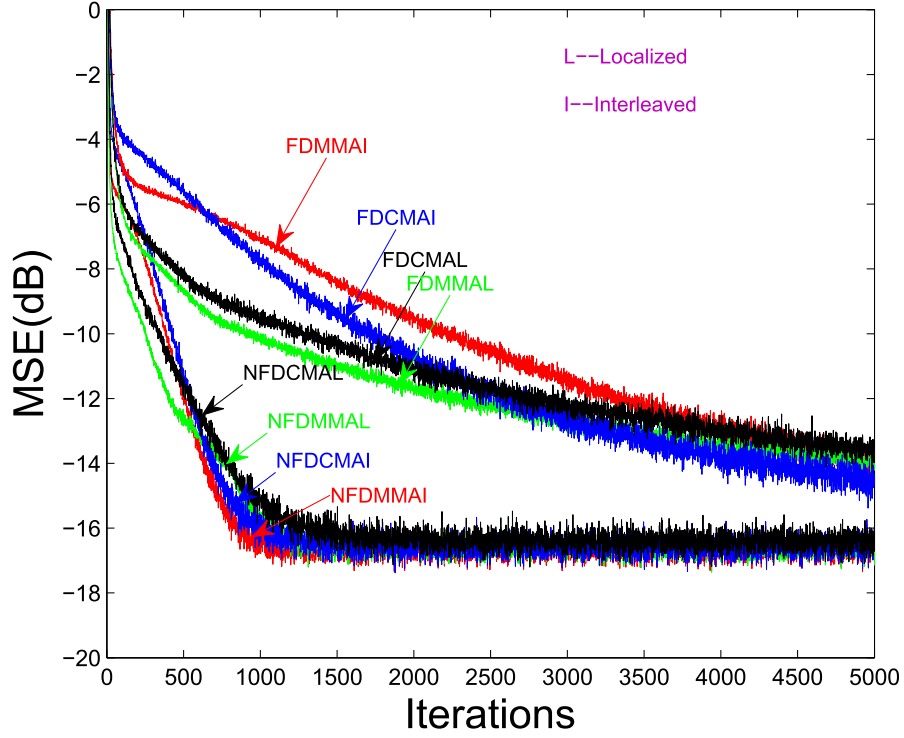


Figure 5.5: MSE comparison curves for FD blind algorithms.

LFDMA. The performance reflect greatly the effect of power normalization on the algorithms convergence rate taking about 1500 symbols for convergence. This correspond to almost 93% improvement in symbols saving over the algorithms without normalization.

Figure 5.5 shows both normalized and unnormalized algorithms for better comparison. It should be noted that the gain in performance comes at a small cost of additional processing in the form of power normalization.

Figure 5.6 and Figure 5.7 show MSE convergence comparison between normalized and unnormalized version for localized mapping scheme and different SNRs. Two more SNR scenarios of 10dB and 30dB are considered. At low SNR of 10dB,

MMA outperformed CMA while both normalized and unnormalized version of each of the algorithms converge to the same residual MSE. MMA algorithms converge to about 9.5dB while CMA converge to about 8.5dB. This shows that MMA has better performance than CMA at low SNR while the effect of normalization is not as significant compared to 20dB scenario. At high SNR of 30dB, the effect of normalization is very significant as the unnormalized version of the algorithms fail to converge at about 5000 iterations while the normalized versions converge at about 2000 iterations. Furthermore, both CMA and MMA converge to the same residual MSE showing that they both have similar performance at high SNR.

Figure 5.8 and Figure 5.9 show MSE convergence comparison between the

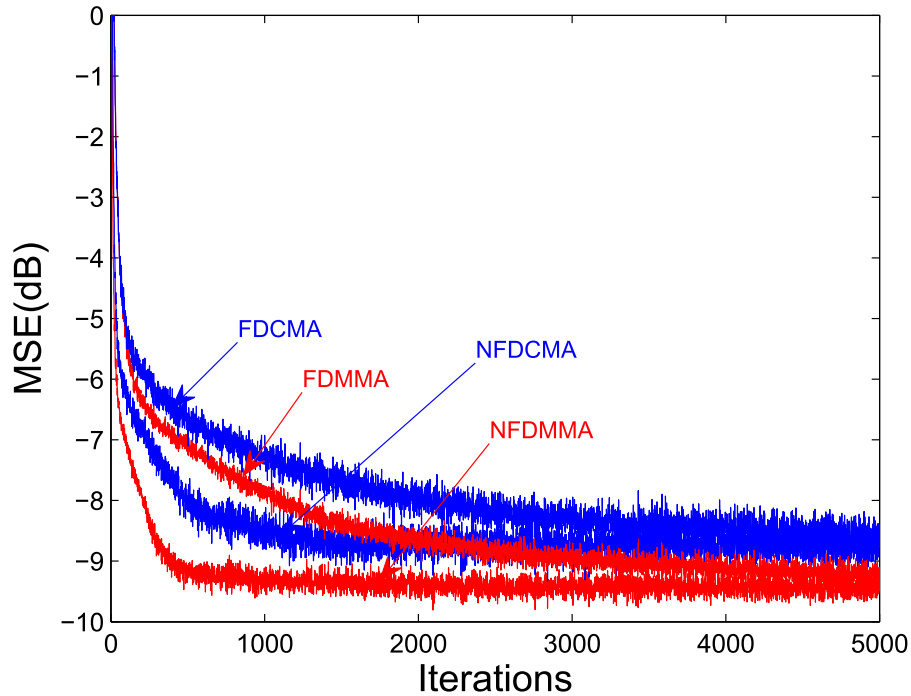


Figure 5.6: MSE comparison curves for FD blind algorithms, SNR=10dB.

mapping schemes and the normalized algorithms respectively. It is seen that

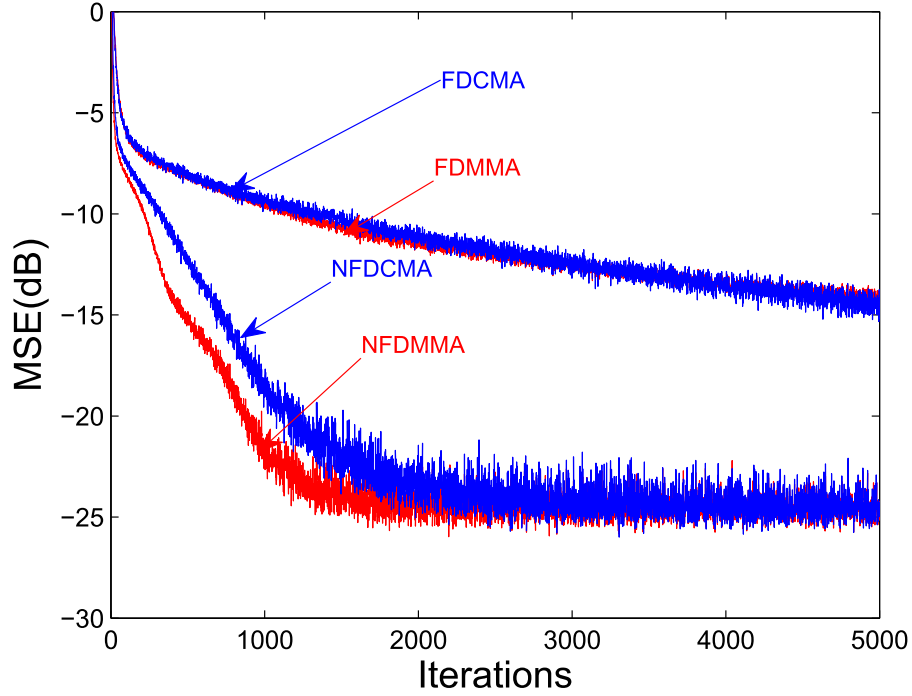


Figure 5.7: MSE comparison curves for FD blind algorithms, SNR=30dB.

though both mapping schemes achieve same residual error, IFDMA achieve a slightly better performance in terms of convergence rate compared to LFDMA which is due to frequency diversity offered to the users. Frequency diversity can be incorporated into LFDMA to improve its performance by implementing channel-dependent scheduling [54]. Also, NFDMMMA converge a little bit faster than NFDCMA which may be due to its ability to perform phase recovery, something not inherent to NFDCMA.

Figure 5.10 shows the phase recovery capability of NFDMMMA. It is seen that NFDCMA is not able to correct the phase rotation introduced by the channel and that NFDMMMA does this perfectly. Indeed, this effect has been observed in numerous time-domain implementations [33], [34] and [55] and as is shown

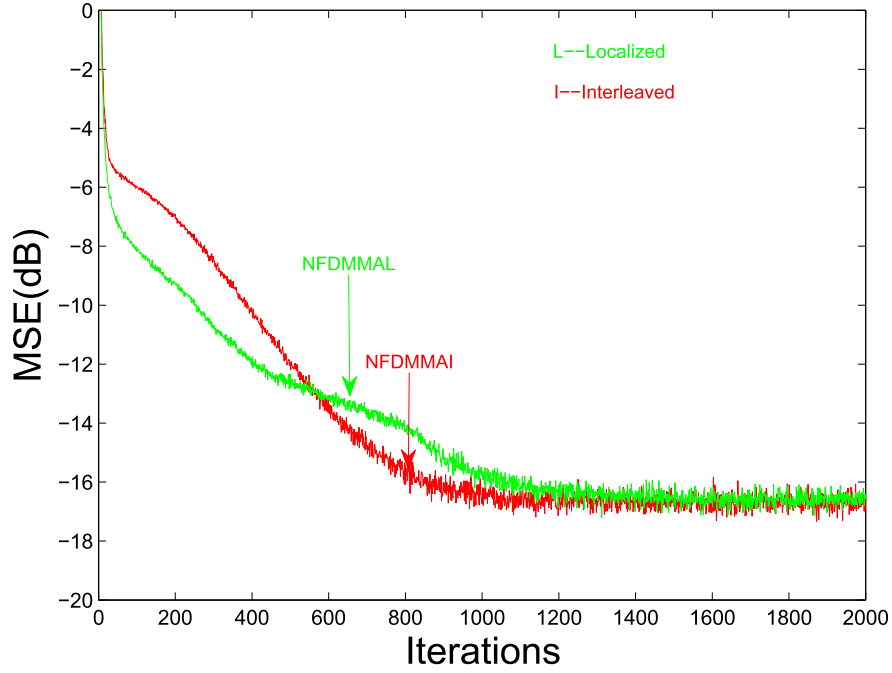


Figure 5.8: MSE comparison curves for mapping scheme.

here, MMA still maintain this ability for frequency domain implementation. The channel in [55] which introduces an arbitrary phase rotation has been used to investigate this phenomenon.

Based on the results of experiment 1, some conclusions were made as follows:

1. SC-FDMA can be equalized with blind frequency domain algorithms as evidenced from the simulation reports above.
2. The normalized version of frequency domain blind algorithms performed better compared to the unnormalized version.
3. Localized SC-FDMA will be studied partly due to the fact that there is not much difference in performance compared to interleaved SC-FDMA and also because 3GPP has chosen it for their uplink SC-FDMA and discontinued

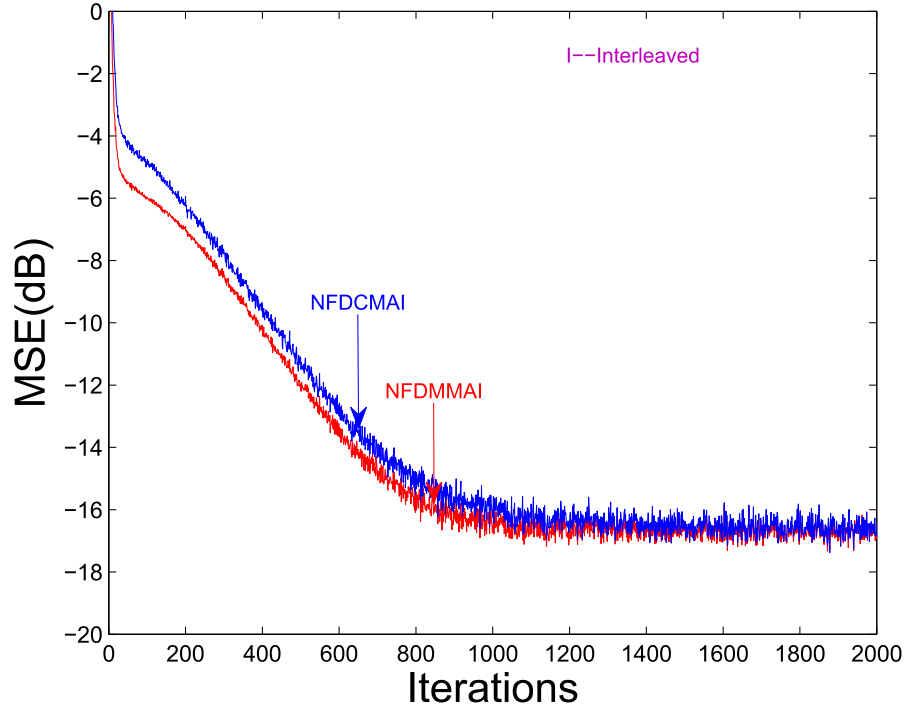


Figure 5.9: MSE comparison curves for normalized FD blind algorithms.

support for IFDMA in 3GPP LTE standard [3], [6], [56].

Therefore subsequent simulations are done in accordance with these conclusions.

5.3.2 Experiment 2

We have evaluated the performance of both frequency domain soft-constraint multimodulus algorithm(FDSCS-MMA) and normalized FDSCS-MMA and compared their performance with the well-known constant modulus algorithm CMA and its modified version MMA . The modulation scheme employed for SC-FDMA transmission is 4QAM. The localized carrier transmission mode is used in LTE uplink since it offers much better performance with the arrangement of pulse-shaping

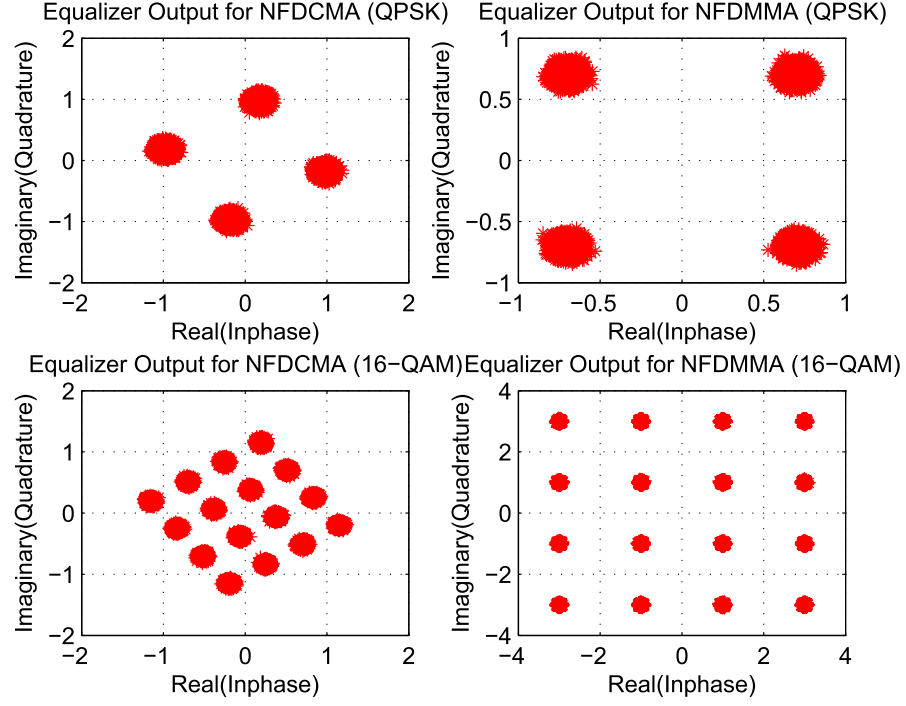


Figure 5.10: Constellation without a carrier offset.

filter. Simulation results are done for LFDMA since DFDMA is no longer supported in 3GPP LTE standard [6]. The values of $R_{2,R}$, $R_{2,I}$ and λ are 1, 1 and 0.55 respectively. The step size for the equalizers are 4×10^{-3} , 3×10^{-3} , 3×10^{-4} and 1×10^{-4} for NFDSCS-MMA, FDSCS-MMA, NFDMA and NFDMA respectively. The channel considered is frequency selective with 6-paths and each path fades independently, according to Rayleigh distribution. Vehicular speed of 1×10^{-4} is used to account for time variation in the channel. The additive white Gaussian noise has been chosen such that the signal to noise ratio at the input of the equalizer is 20 dB.

Figure 5.12 shows performance of NFDSCS-MMA and FDSCS-MMA. The two algorithms achieve the same residual MSE but have different convergence

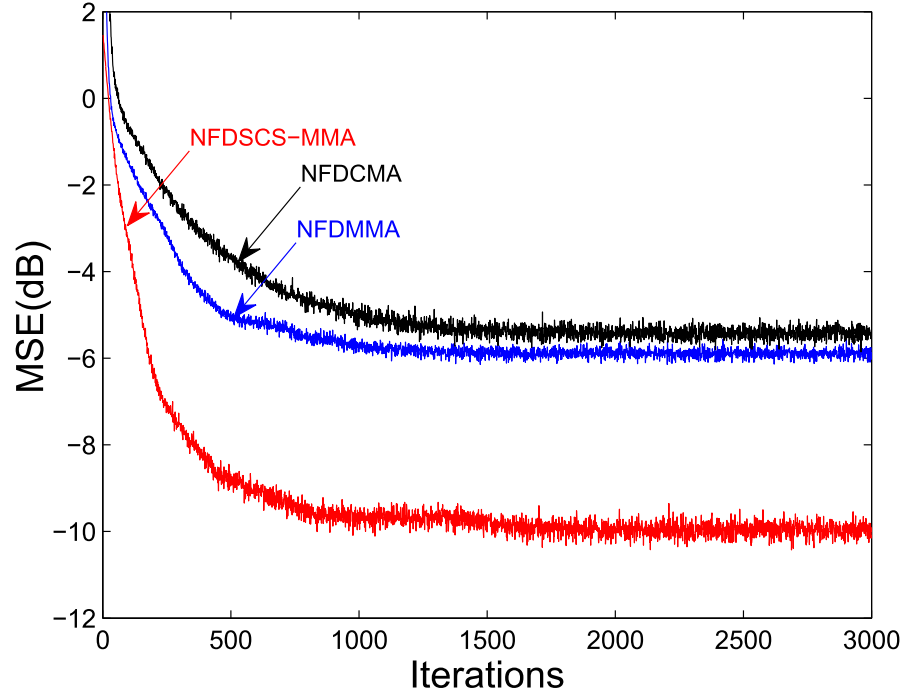


Figure 5.11: MSE comparison curves for blind algorithms, SNR=10dB.

time. It is seen that FDSCS-MMA took a longer time to converge, about 3,000 symbols. This slow adaptation is a setback in broadband wireless communication system which typically require high speed transmission. The convergence rate was then improved greatly by considering a normalization factor leading to NFDSCS-MMA which converges at about 500 symbols. This corresponds to almost 83% improvement in symbols saving over the algorithm without normalization for the same residual MSE. It can be deduced from the curves in Fig 5.12 that the effect of appropriate normalization is to provide better convergence seeing that even though NFDMMMA and NFDCMA have higher residual MSE than FDSCS-MMA, they both have better convergence rate due to their normalization.

Figure 5.11 shows MSE convergence comparison between the proposed nor-

malized algorithms at low SNR of 10dB. NFDSCS-MMA clearly has faster MSE convergence and lower residual MSE compare to other normalized blind algorithms. This shows superior performance of the proposed algorithms at low SNR.

Figure 5.13 shows MSE convergence comparison between the proposed algorithms and the well-known CMA and MMA. Normalised FDCMA and FDMMA are considered because they converge faster than their unnormalized counterparts as has been shown in section 5.3. FDSCS-MMA has a lower MSE but its convergence is slower than that of NFDCMA and NFDMMMA however NFDSCS-MMA is better both in terms of convergence rate and MSE level attained.

Figure 5.14, Figure 5.15 and Figure 5.16 show ISI convergence comparison

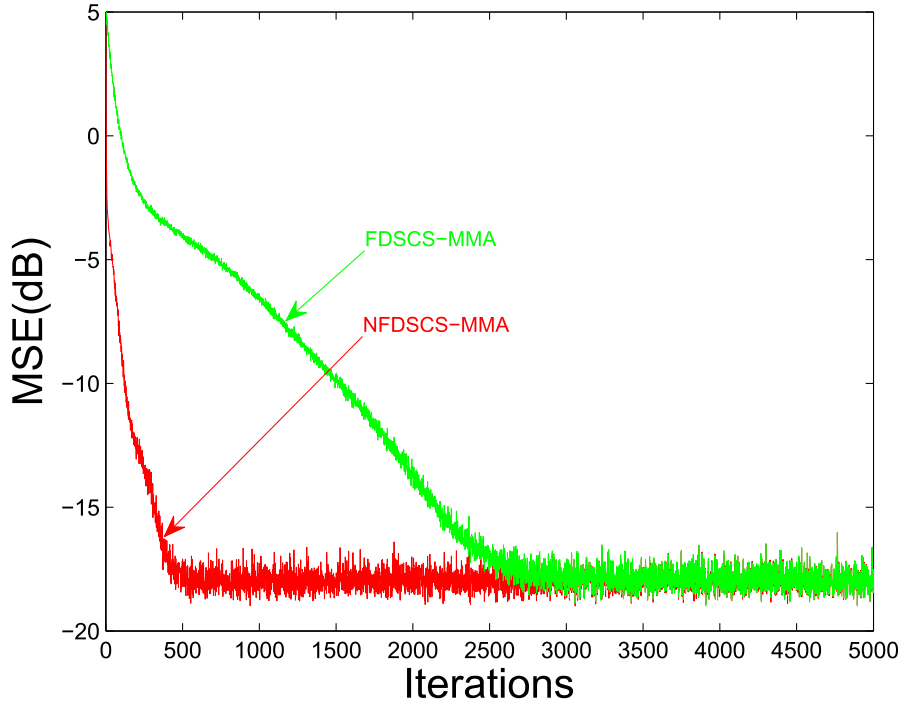


Figure 5.12: MSE curves comparison between NFDSCS-MMA and FDSCS-MMA, SNR=20dB.

between NFDSCS-MMA, NFDMMMA and NFDCMA for different SNR scenarios

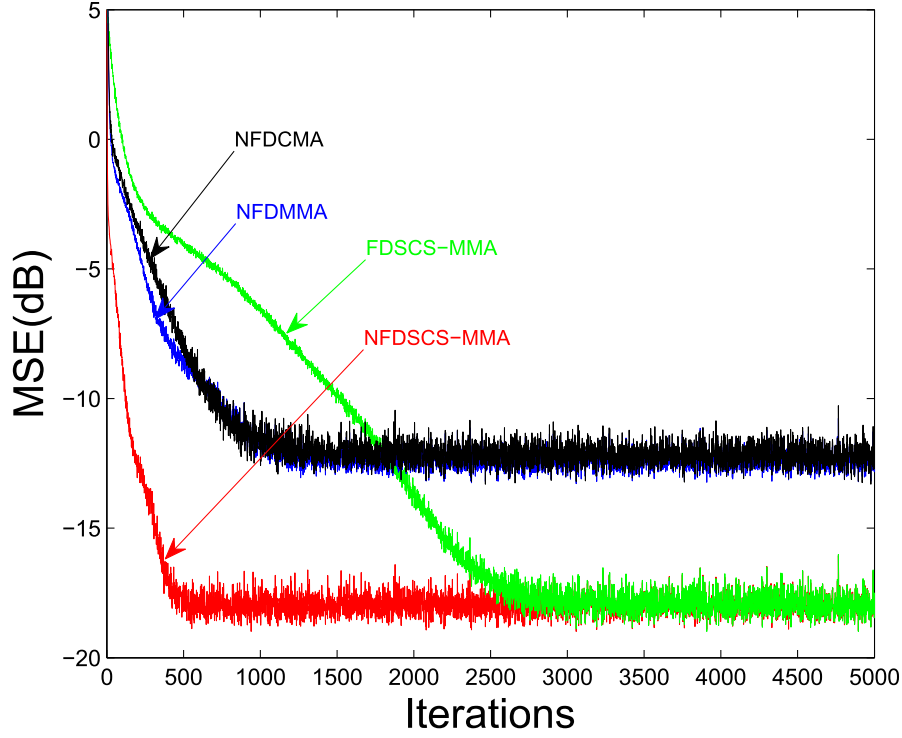


Figure 5.13: MSE comparison curves for blind algorithms, SNR=20dB.

using 4-QAM. NFDSCS-MMA has the fastest convergence while all of the algorithms converge to the same residual ISI. Convergence rate decreases slightly with increase in SNR such that faster convergence is recorded at lower SNR though high SNR result in lower residual ISI.

Figure 5.17 shows the residual ISI for the proposed algorithm and other blind algorithms for higher constellation order of 64-QAM. It is seen that FDSCS-MMA is very slow to converge while NFDSCS-MMA achieve the least residual ISI with approximately 3-dB improvements over NFDSCMA and NFDMMMA.

Figure 5.18 shows the phase recovery capability of NFDSCS-MMA. It is seen that NFDSCMA is not able to correct the phase rotation introduced by channel characteristics and that both NFDMMMA and NFDSCS-MMA do this perfectly.

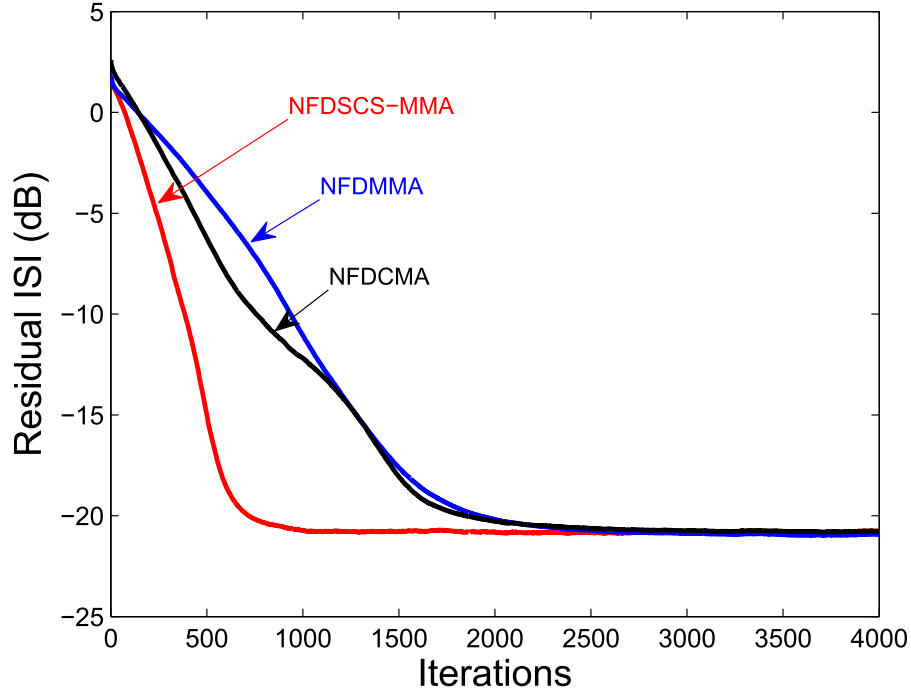


Figure 5.14: Residual ISI convergence curves for 4-QAM for blind algorithms, SNR=10dB.

This is due to the fact that both equalizers achieve equalization by forcing both the real and imaginary parts of the equalizer output onto four-point contours thereby simultaneously perform blind equalization and carrier phase recovery. The channel in [55] which introduces an arbitrary phase rotation has been used to investigate this phenomenon.

Figure 5.19 shows the ability of the developed algorithms to open the eye of a 64-QAM constellation. It is seen that normalized FDSCS-MMA has a better constellation recovery capability than its unnormalized version for the same iteration period.

Figure 5.20 shows the BER performance of both FDSCS-MMA with its normalized version compared to linear optimum equalizers which are minimum

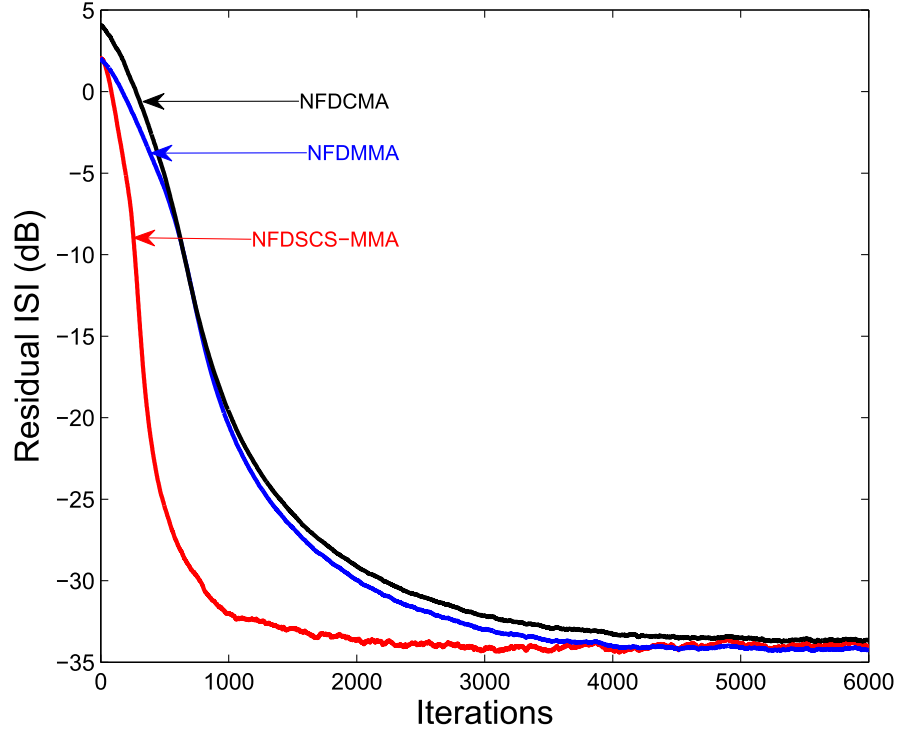


Figure 5.15: Residual ISI convergence curves for 4-QAM for blind algorithms, SNR=20dB.

mean square (linear MMSE) and zero forcing equalizers. In order to assess the BER performance of NFDSCS-MMA, knowledge of the first 2 received symbols has been assumed since SCS-MMA only minimize the dispersion between real and imaginary parts of the received signal and a four-point contours of distance $R_{2,R:I}$. This assumption is required to correct the received signal phase [12] as "blind" in blind equalizers is with respect to the phase hence, they are said to be blind to the "phase". It is shown in Fig 5.20 that both NFDSCS-MMA and FDSCS-MMA achieve similar BER performance which is slightly less than that of linear MMSE. In situations where blind equalizers are used to open the eye of the signal constellation, a probability of symbol error of 10^{-2} is considered acceptable [33].

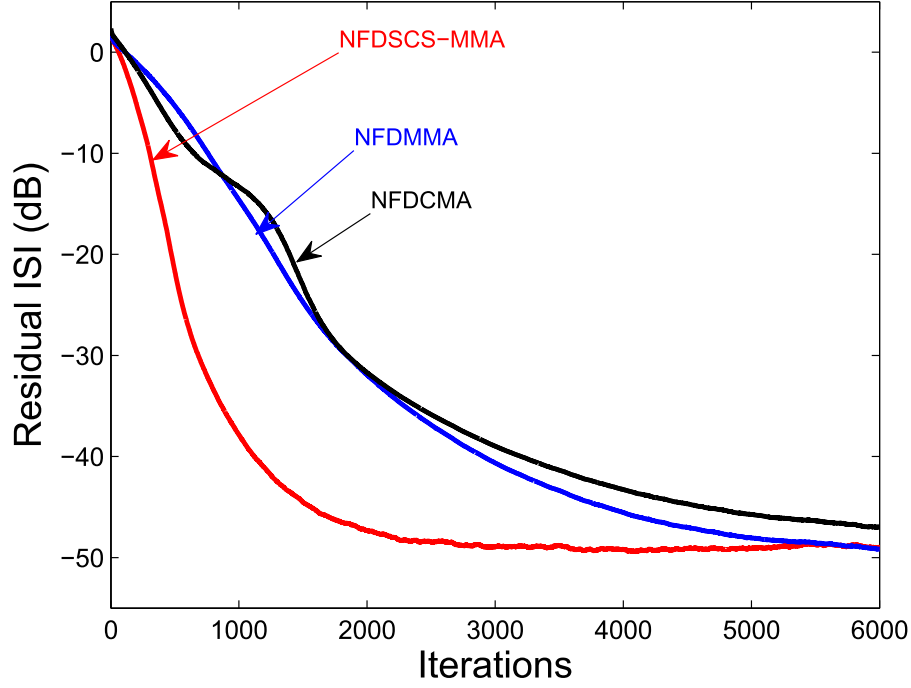


Figure 5.16: Residual ISI convergence curves for 4-QAM for blind algorithms, SNR=30dB.

From figure 5.20, it is seen that to achieve this acceptable performance, 8dB is required for NFDSCS-MMA as compared to that of 7dB for linear MMSE which is a small tradeoff compare to 14% improvement in throughput achieved by using the proposed algorithm.

5.4 Summary

In this Chapter, we have implemented a novel frequency domain soft-constraint multimodulus algorithm for single carrier. It is shown that the proposed algorithm outperform the popular blind algorithm, CMA and its modified version, MMA in both residual MSE and convergence rate. Phase recovery capability of the

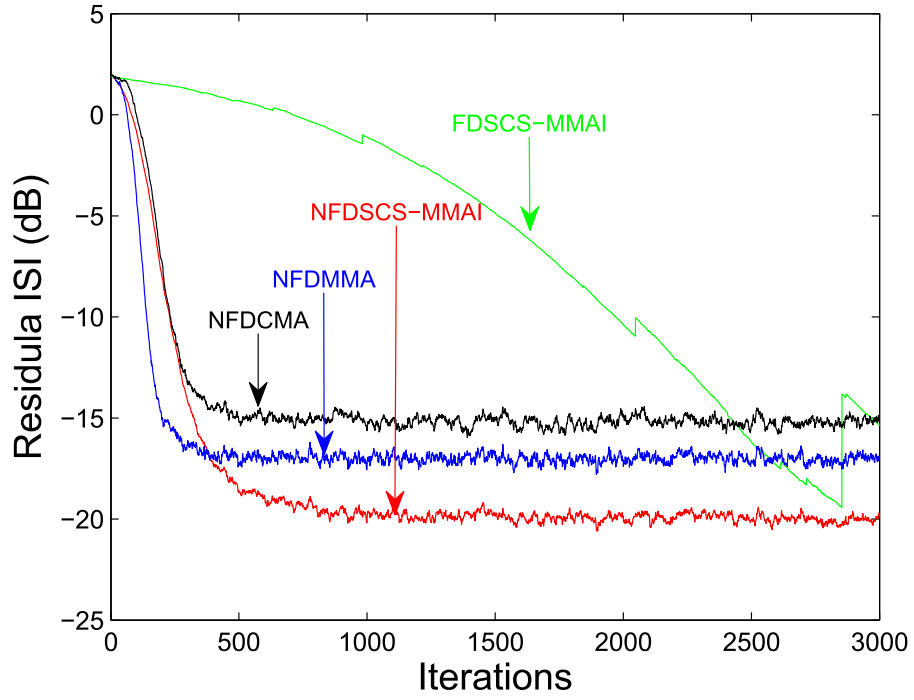


Figure 5.17: Residual ISI convergence curves for 64-QAM for blind algorithms, SNR=20dB.

proposed algorithm is also demonstrated with acceptable BER performance. This suggest that SCFDMA can be perfectly equalized in broadband systems using the proposed algorithm with the resultant lower MSE, faster convergence and improved spectral efficiency.

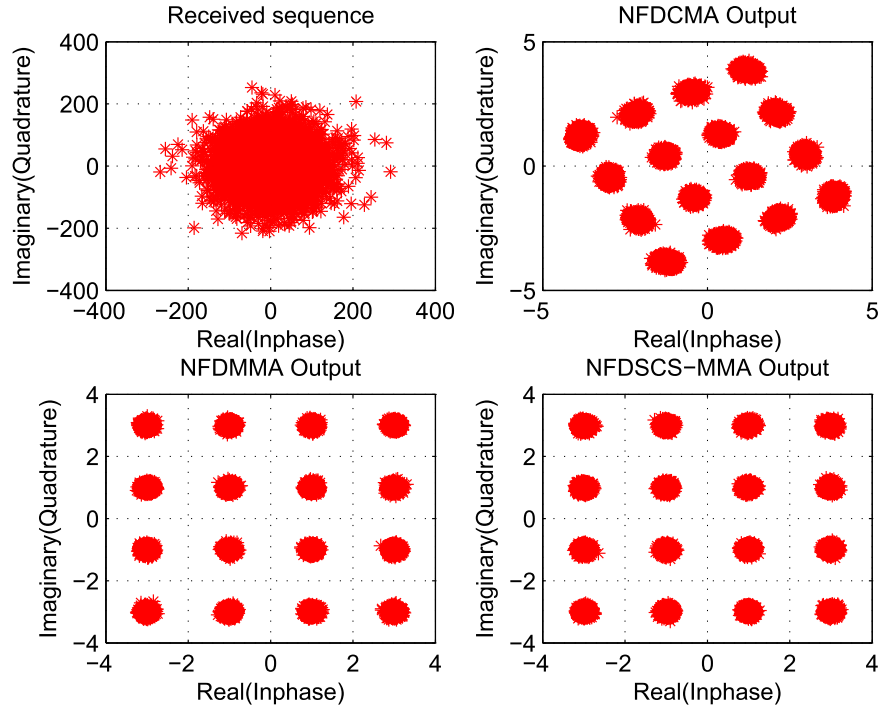


Figure 5.18: Constellation without a carrier offset, SNR=20dB.

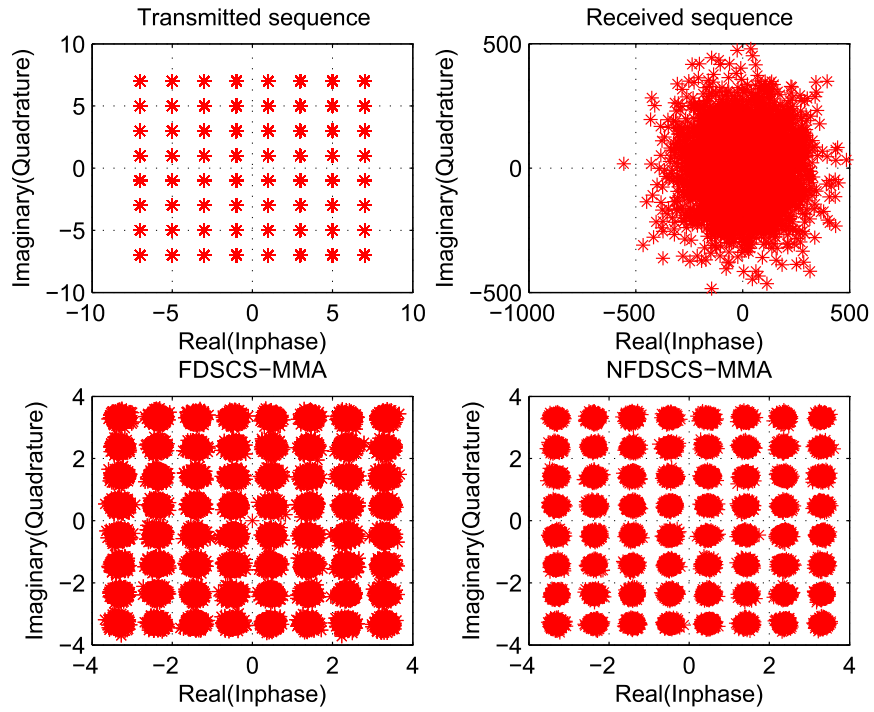


Figure 5.19: Constellation without a carrier offset, SNR=30dB.

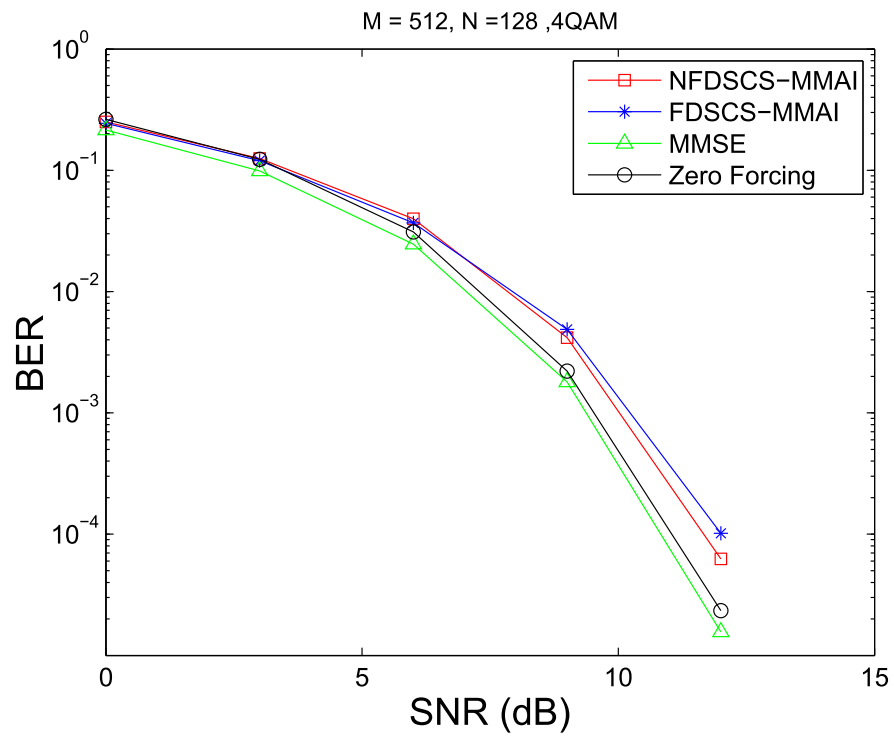


Figure 5.20: BER comparison of NFDSCS-MMA and Linear MMSE.

CHAPTER 6

CONCLUSION AND FUTURE WORK

6.1 Conclusion

In this work, we have developed and implemented a frequency domain soft-constraint multimodulus (FDSCS-MMA) algorithm for uplink SC-FDMA. The algorithm performance is then enhanced by normalization technique to realize normalized FDSCS-MMA (NFDSCS-MMA). The proposed NFDSCS-MMA outperformed its time-domain counterpart, SCS-MMA, in terms of lower complexity, lower residual MSE and faster convergence rate with similar residual ISI and BER performance. The proposed NFDSCS-MMA is further adapted to SC-FDMA equalization to improve throughput degradation in uplink SC-FDMA. It is shown that NFDSCS-MMA outperform both NFDCMA and NFDMMMA in both residual MSE and convergence rate. Phase recovery capability of the proposed algorithm

is also demonstrated. Finally, NFDSCS-MMA was shown to achieve slightly lower BER performance compared to optimum MMSE. This suggest that SC-FDMA can be perfectly equalized in broadband systems using the proposed algorithm with increase in spectral efficiency and significant throughput improvement.

6.2 Future work

Further work can be done in the following areas:

- Implement decision feedback approach for the proposed algorithm.
- Investigate other transforms to reduce further the computational complexity.
- Use non-power-of-two Radix FFT algorithms to accommodate real time scenarios.
- Use of blind fractionally spaced equalizers in frequency domain.

REFERENCES

- [1] J. A. C. Bingham, “Multicarrier modulation for data transmission: an idea whose time has come,” *Communications Magazine, IEEE*, vol. 28, no. 5, pp. 5–14, 1990.
- [2] K. Paterson, “Generalized reed-muller codes and power control in ofdm modulation,” *Information Theory, IEEE Transactions on*, vol. 46, no. 1, pp. 104–120, Jan 2000.
- [3] H. G. Myung and D. J. Goodman, *Single Carrier FDMA: A New Air Interface for Long Term Evolution*. John Wiley and Sons, Inc.
- [4] H. Myung, J. Lim, and D. Goodman, “Single carrier fdma for uplink wireless transmission,” *Vehicular Technology Magazine, IEEE*, vol. 1, no. 3, pp. 30–38, Sept 2006.
- [5] N. Benvenuto, R. Dinis, D. Falconer, and S. Tomasin, “Single carrier modulation with nonlinear frequency domain equalization: An idea whose time has come again,” *Proceedings of the IEEE*, vol. 98, no. 1, pp. 69–96, 2010.

- [6] G. Huang, A. Nix, and S. Armour, "Decision feedback equalization in sc-fdma," in *Personal, Indoor and Mobile Radio Communications, 2008. PIMRC 2008. IEEE 19th International Symposium on*, Sept 2008, pp. 1–5.
- [7] S. Yameogo, J. Palicot, and L. Cariou, "Blind time domain equalization of scfdma signal," in *Vehicular Technology Conference Fall (VTC 2009-Fall), 2009 IEEE 70th*, Sept 2009, pp. 1–4.
- [8] H. G. Myung, *3Gpp Long Term Evolution: A Technical Overview*. John Wiley & Sons, Inc., 2010.
- [9] S. Abrar, A. Zerguine, and M. Deriche, "Soft constraint satisfaction multimodulus blind equalization algorithms," *Signal Processing Letters, IEEE*, vol. 12, no. 9, pp. 637–640, Sept 2005.
- [10] J.-C. Lin, "Blind equalisation technique based on an improved constant modulus adaptive algorithm," *Communications, IEE Proceedings-*, vol. 149, no. 1, pp. 45–50, Feb 2002.
- [11] N. Bershad and P. Feintuch, "A normalized frequency domain lms adaptive algorithm," *Acoustics, Speech and Signal Processing, IEEE Transactions on*, vol. 34, no. 3, pp. 452–461, Jun 1986.
- [12] H. H. Dam, S. Nordholm, and H. Zepernick, "Frequency domain constant modulus algorithm for broadband wireless systems," in *Global Telecommunications Conference, 2003. GLOBECOM '03. IEEE*, vol. 1, Dec 2003, pp. 40–44 Vol.1.

- [13] D. H. Carlson, “Review: Philip j. davis, circulant matrices,” *Bulletin (New Series) of the American Mathematical Society*, vol. 7, no. 2, pp. 421–422, 09 1982. [Online]. Available: <http://projecteuclid.org/euclid.bams/1183549650>
- [14] H. Witschnig, M. Kemptner, R. Weigel, and A. Springer, “Decision feedback equalization for a single carrier system with frequency domain equalization - an overall system approach,” in *Wireless Communication Systems, 2004, 1st International Symposium on*, 2004, pp. 26–30.
- [15] D. Falconer, S. Ariyavisitakul, A. Benyamin-Seeyar, and B. Eidson, “Frequency domain equalization for single-carrier broadband wireless systems,” *Communications Magazine, IEEE*, vol. 40, no. 4, pp. 58–66, Apr 2002.
- [16] Y. Zhu, C. Li, and G. Zheng, “A Study of Channel Estimation in Multi-Band OFDM UWB Systems,” *Communications*, 2007. [Online]. Available: <http://epress.lib.uts.edu.au/dspace/handle/2100/69>
- [17] N. Benvenuto and S. Tomasin, “Iterative design and detection of a dfe in the frequency domain,” *Communications, IEEE Transactions on*, vol. 53, no. 11, pp. 1867–1875, 2005.
- [18] C. Zhang, Z. Wang, Z. Yang, J. Wang, and J. Song, “Frequency domain decision feedback equalization for uplink sc-fdma,” *Broadcasting, IEEE Transactions on*, vol. 56, no. 2, pp. 253–257, June 2010.

- [19] S. Yameogo, P. Jacques, and L. Cariou, "A semi-blind time domain equalization of scfdma signal," in *Signal Processing and Information Technology (ISSPIT), 2009 IEEE International Symposium on*, Dec 2009, pp. 360–365.
- [20] S. Yameogo and J. Palicot, "Frequency domain equalization of sc-fdma signal without any reference symbols," in *Consumer Electronics, 2009. ICCE '09. Digest of Technical Papers International Conference on*, Jan 2009, pp. 1–2.
- [21] N. Iqbal, N. Al-Dhahir, A. Zerguine, and A. Zidouri, "Adaptive frequency-domain rls dfe for uplink mimo sc-fdma," *Vehicular Technology, IEEE Transactions on*, vol. PP, no. 99, pp. 1–1, 2014.
- [22] G.-H. Im and J.-J. Werner, "Bandwidth-efficient digital transmission over unshielded twisted-pair wiring," *Selected Areas in Communications, IEEE Journal on*, vol. 13, no. 9, pp. 1643–1655, Dec 1995.
- [23] D. Harman, G. Huang, G.-H. Im, M.-H. Nguyen, J.-J. Werner, and M. Wong, "Local distribution for interactive multimedia tv to the home," in *Community Networking Integrated Multimedia Services to the Home, 1994., Proceedings of the 1st International Workshop on*, Jul 1994, pp. 175–182.
- [24] —, "Local distribution for imtv," *MultiMedia, IEEE*, vol. 2, no. 3, pp. 14–23, Autumn 1995.
- [25] G.-H. Im, D. Harman, G. Huang, A. Mandzik, M.-H. Nguyen, and J.-J. Werner, "51.84 mb/s 16-cap atm lan standard," *Selected Areas in Communications, IEEE Journal on*, vol. 13, no. 4, pp. 620–632, May 1995.

- [26] N. Benvenuto and T. Goeddel, "Classification of voiceband data signals using the constellation magnitude," *Communications, IEEE Transactions on*, vol. 43, no. 11, pp. 2759–2770, Nov 1995.
- [27] J. Treichler, C. Johnson, and M. Larimore, *Theory and design of adaptive filters*, ser. Topics in digital signal processing. Wiley, 1987. [Online]. Available: <http://books.google.com.sa/books?id=KR5TAAAAMAAJ>
- [28] D. Godard, "Self-recovering equalization and carrier tracking in two-dimensional data communication systems," *Communications, IEEE Transactions on*, vol. 28, no. 11, pp. 1867–1875, Nov 1980.
- [29] J. Treichler and B. Agee, "A new approach to multipath correction of constant modulus signals," *Acoustics, Speech and Signal Processing, IEEE Transactions on*, vol. 31, no. 2, pp. 459–472, Apr 1983.
- [30] J. Litwin, L.R., "Blind channel equalization," *Potentials, IEEE*, vol. 18, no. 4, pp. 9–12, Oct 1999.
- [31] J. Johnson, R., P. Schniter, T. Endres, J. Behm, D. Brown, and R. Casas, "Blind equalization using the constant modulus criterion: a review," *Proceedings of the IEEE*, vol. 86, no. 10, pp. 1927–1950, Oct 1998.
- [32] K. N. Oh and Y. Chin, "Modified constant modulus algorithm: blind equalization and carrier phase recovery algorithm," in *Communications, 1995. ICC '95 Seattle, 'Gateway to Globalization', 1995 IEEE International Conference on*, vol. 1, Jun 1995, pp. 498–502 vol.1.

- [33] J. Yang, J.-J. Werner, and G. Dumont, "The multimodulus blind equalization and its generalized algorithms," *Selected Areas in Communications, IEEE Journal on*, vol. 20, no. 5, pp. 997–1015, Jun 2002.
- [34] J.-T. Yuan and K.-D. Tsai, "Analysis of the multimodulus blind equalization algorithm in qam communication systems," *Communications, IEEE Transactions on*, vol. 53, no. 9, pp. 1427–1431, Sept 2005.
- [35] L. Garth, J. Yang, and J.-J. Werner, "Blind equalization algorithms for dual-mode cap-qam reception," *Communications, IEEE Transactions on*, vol. 49, no. 3, pp. 455–466, Mar 2001.
- [36] O. Tanrikulu, B. Baykal, A. G. Constantinides, and J. A. Chambers, "Soft constraint satisfaction (scs) blind channel equalization algorithms," *International Journal of Adaptive Control and Signal Processing*, vol. 12, no. 2, pp. 117–134, 1998. [Online]. Available: [http://dx.doi.org/10.1002/\(SICI\)1099-1115\(199803\)12:2<117::AID-ACS483>3.0.CO;2-Y](http://dx.doi.org/10.1002/(SICI)1099-1115(199803)12:2<117::AID-ACS483>3.0.CO;2-Y)
- [37] O. Tanrikulu, A. Constantinides, and J. Chambers, "New normalized constant modulus algorithms with relaxation," *Signal Processing Letters, IEEE*, vol. 4, no. 9, pp. 256–258, Sept 1997.
- [38] A. Benveniste and M. Goursat, "Blind equalizers," *Communications, IEEE Transactions on*, vol. 32, no. 8, pp. 871–883, Aug 1984.
- [39] S. Abrar, A. Zerguine, and M. Deriche, "Soft constraint satisfaction multimodulus blind equalization algorithms," in *Acoustics, Speech, and Signal*

- Processing, 2004. Proceedings. (ICASSP '04). IEEE International Conference on*, vol. 2, May 2004, pp. ii–853–6 vol.2.
- [40] S. Abrar and A. Zerguine, “A new multimodulus blind equalization algorithm,” in *Networking and Communication Conference, 2004. INCC 2004. International*, June 2004, pp. 165–169.
- [41] Y. G. Yang, N. I. Cho, and S. U. Lee, “Fast blind equalization by using frequency domain block constant modulus algorithm,” in *Circuits and Systems, 1995., Proceedings., Proceedings of the 38th Midwest Symposium on*, vol. 2, Aug 1995, pp. 1003–1006 vol.2.
- [42] J. Salz and S. B. Weinstein, “Fourier transform communication system,” in *Proceedings of the First ACM Symposium on Problems in the Optimization of Data Communications Systems*. New York, NY, USA: ACM, 1969, pp. 99–128. [Online]. Available: <http://doi.acm.org/10.1145/800165.805240>
- [43] S. Weinstein and P. Ebert, “Data transmission by frequency-division multiplexing using the discrete fourier transform,” *Communication Technology, IEEE Transactions on*, vol. 19, no. 5, pp. 628–634, October 1971.
- [44] G. Clark, S. Parker, and S. Mitra, “A unified approach to time- and frequency-domain realization of fir adaptive digital filters,” *Acoustics, Speech and Signal Processing, IEEE Transactions on*, vol. 31, no. 5, pp. 1073–1083, Oct 1983.

- [45] Y. yuan Kong, "A cma equalization system in frequency domain," in *Communication Technology (ICCT), 2010 12th IEEE International Conference on*, Nov 2010, pp. 358–360.
- [46] Y. G. Yang, C. H. Park, and J. Song, "Fast constant modulus algorithm in the dft domain," in *Radio and Wireless Conference, 2004 IEEE*, Sept 2004, pp. 19–22.
- [47] M. M. Usman Gul and S. A. Sheikh, "Design and implementation of a blind adaptive equalizer using frequency domain square contour algorithm," *Digit. Signal Process.*, vol. 20, no. 6, pp. 1697–1710, Dec. 2010. [Online]. Available: <http://dx.doi.org/10.1016/j.dsp.2010.03.013>
- [48] T. Walzman and M. Schwartz, "Automatic equalization using the discrete frequency domain," *Information Theory, IEEE Transactions on*, vol. 19, no. 1, pp. 59–68, Jan 1973.
- [49] C. Chan, M. Petraglia, and J. Shynk, "Frequency-domain implementations of the constant modulus algorithm," in *Signals, Systems and Computers, 1989. Twenty-Third Asilomar Conference on*, vol. 2, 1989, pp. 663–669.
- [50] A. V. Oppenheim, R. W. Schafer, and J. R. Buck, *Discrete-time Signal Processing (2Nd Ed.)*. Upper Saddle River, NJ, USA: Prentice-Hall, Inc., 1999.
- [51] A. H. Sayed, *Adaptive Filters*. Wiley-IEEE Press, 2008.
- [52] P. Duhamel and M. Vetterli, "Fast fourier transforms: A tutorial review and a state of the art," *Signal Processing*,

- p. 259 – 299, 1990. [Online]. Available:
-
- <http://www.sciencedirect.com/science/article/pii/016516849090158U>
- [53] O. Shalvi and E. Weinstein, “New criteria for blind deconvolution of nonminimum phase systems (channels),” *Information Theory, IEEE Transactions on*, vol. 36, no. 2, pp. 312–321, Mar 1990.
- [54] J. Lim, H. Myung, K. Oh, and D. Goodman, “Channel-dependent scheduling of uplink single carrier fdma systems,” in *Vehicular Technology Conference, 2006. VTC-2006 Fall. 2006 IEEE 64th*, Sept 2006, pp. 1–5.
- [55] C. Li, W. Dong, G. Wan, and L. Chen, “A new multi-modulus blind equalization algorithm for qam signals,” in *Wireless Communications, Networking and Mobile Computing, 2009. WiCom '09. 5th International Conference on*, Sept 2009, pp. 1–4.
- [56] F. E. Abd El-Samie, F. S. Al-kamali, A. Y. Al-nahari, and M. I. Dessouky, *SC-FDMA for Mobile Communications*. Boca Raton, FL, USA: CRC Press, Inc., 2013.

Vitae

- Name: Kabiru Akande Oluwaseun
- Nationality: Nigerian
- Date of Birth: May 07,1983
- Email: *koakande@gmail.com*
- Permenant Address: 16 Oluwasesan Adekoya Street, Off Ailegbe Road, Ejigbo, Lagos, Nigeria
- Academic Background:
 - MS in Electrical Engineering, King Fahd University of Petroleum and Minerals, KFUPM, Dhahran, KSA.
 - B.Tech in Electronics and Electrical Engineering, Ladoke Akintola University of Technology, Ogbomoso, Nigeria.
- Publications:
 - **K. Akande**, N. Iqbal and A. Zerguine "Frequency Domain Soft-Constraint Satisfaction Multimodulus Blind Algorithm" Prepared for IET ELECTRONICS LETTER.

- **Kabiru Akande**, Naveed Iqbal, Azzedine Zerguine, Naofal Al-Dhahir and Abdelmalek Zidouri "Frequency Domain Soft-Constraint Multi-modulus Blind Equalization for Uplink SC-FDMA" Under preparation.